Frontiers in Bioscience Landmark

Front. Biosci. (Landmark Ed) **2025**; 30(10): 44677
https://doi.org/10.31083/FBL44677

Original Research

Calcitonin Alleviates Sepsis-Induced Acute Lung Injury by Inhibiting the HMGB1/MyD88/NF-κB Pathway by Targeting CD3D

Hongyan Zhang[1,*,†], Ruiqing Zong[1,†], Huiqi Wu[1], Jun Jiang[2], Jian He[3,*]

[1]Department of Critical Care Medicine, The Third Affiliated Hospital of Naval Medical University, 201805 Shanghai, China
[2]State Key Laboratory of Genetic Engineering, Shanghai Engineering Research Center of Industrial Microorganisms, School of Life Sciences, Fudan University, 200438 Shanghai, China
[3]Department of Critical Care Medicine and Emergency Medicine, The Third Affiliated Hospital of Naval Medical University, 201805 Shanghai, China
*Correspondence: 13681639049@139.com (Hongyan Zhang); 13386273919@126.com (Jian He)
[†]These authors contributed equally.

Academic Editors: Graham Pawelec and Vijay Kumar
Submitted: 9 July 2025 Revised: 13 September 2025 Accepted: 22 September 2025 Published: 28 October 2025

Abstract

Background: Acute lung injury (ALI) triggered by sepsis continues to pose a significant difficulty in clinical practice. Due to its anti-inflammatory and antioxidant activities, calcitonin is considered a potential therapeutic option in sepsis. **Methods**: Bioinformatics analysis was performed using the GSE89376 and GSE67652 datasets. Serum levels of *CD3D* and NLR family pyrin domain containing 3 (NLRP3) inflammasome, as well as high-mobility group box 1 (HMGB1)/myeloid differentiation primary response gene 88 (MyD88)/nuclear factor-κB (NF-κB) pathway components, were evaluated in sepsis/ALI patients. The effects of calcitonin and *CD3D* knockdown on human pulmonary microvascular endothelial cells (hPMECs) activated by lipopolysaccharide (LPS) were investigated *in vitro*. Experimental assays, including quantitative real-time polymerase chain reaction (qRT-PCR), Cell Counting Kit-8 (CCK-8) assay, western blotting (WB), enzyme-linked immunosorbent assay (ELISA), and flow cytometry, were used to assess cell viability, apoptosis, cell cycle, and oxidative stress markers. **Results**: *CD3D* was identified as a key sepsis/ALI-associated hub gene and correlated with NF-κB pathway activation in patients. *CD3D* silencing in hPMECs effectively suppressed LPS-induced inflammation, oxidative stress, apoptosis, and G1 phase arrest by downregulating the expression of NLRP3, phosphorylation (p)-NF-κB, MyD88, and HMGB1. Calcitonin alone mitigated LPS-induced injury in a dose-dependent way and further enhanced the protective impacts of *CD3D* knockdown. Co-treatment resulted in synergistic inhibition of interleukin (IL)-1β, IL-6, and tumor necrosis factor (TNF)-α, a reduction in oxidative markers, restoration of antioxidant capacity (superoxide dismutase (SOD) and glutathione (GSH)), improved endothelial cell viability, and attenuation of apoptosis. Notably, combined treatment more robustly suppressed the HMGB1/MyD88/NF-κB pathway than either intervention alone. **Conclusion**: *CD3D* exacerbates sepsis-induced ALI by potentiating the HMGB1/MyD88/NF-κB pathway and NLRP3 inflammasome, driving inflammation and oxidative stress. Combined *CD3D* knockdown and calcitonin treatment offers a novel synergistic therapeutic strategy for mitigating pulmonary endothelial injury in sepsis.

Keywords: calcitonin; sepsis; acute lung injury; *CD3D*; HMGB1; MyD88; NF-κB

1. Introduction

Sepsis is a reaction of systemic inflammation triggered by invading pathogenic microorganisms such as bacteria. Its risk factors are diverse and include advanced age, immunosuppression, chronic comorbidities, and invasive medical procedures [1]. The acute systemic inflammation associated with sepsis frequently involves the respiratory system, with the lungs being particularly vulnerable [2]. Excessive inflammation and oxidative stress during sepsis contribute to the development of acute lung injury (ALI) and acute respiratory distress syndrome (ARDS), conditions characterized by severe outcomes and elevated mortality [3]. Additionally, acute inflammation in sepsis induces oxidative stress, which disrupts endothelial cell function and causes microvascular dysfunction [4]. Such alterations in endothelial responses promote pathological processes, including inflammation, coagulation, and cell adhesion, ultimately contributing to organ dysfunction [5]. Recent experimental evidence has demonstrated that oleuropein exerts protective effects against lipopolysaccharide (LPS)-induced ALI in rats through anti-inflammatory and antioxidant mechanisms [6], while a meta-analysis has highlighted the efficacy of terpenoids in reducing pulmonary edema in ALI animal models, supporting the therapeutic potential of natural compounds [7]. Furthermore, accumulating evidence suggests that antioxidant-based interventions may exert protective effects in sepsis, highlighting their promising therapeutic potential [8,9]. Therefore, the development of innovative therapeutic strategies and reliable prognostic biomarkers is crucial for improving clinical outcomes in patients with sepsis.

Procalcitonin (PCT) is widely recognized as one of the most specific and sensitive biomarkers for diagnosing sepsis [10]. PCT, the prohormone of calcitonin, is generally processed by enzymatic cleavage to yield mature calcitonin

and several smaller peptide fragments [11]. Calcitonin, a peptide hormone secreted primarily by the thyroid gland, is crucial in modulating calcium and phosphate metabolism [12]. Evidence suggests that severe infections and sepsis can induce skeletal destruction, tissue injury, and other physiological abnormalities, which may in turn elevate circulating calcium concentrations [13]. In such conditions, calcitonin functions to decrease circulating calcium concentrations through the inhibition of calcium release. Notably, studies in animal models and *ex vivo* human blood have demonstrated that calcitonin exerts a modest but deleterious effect in experimental septic shock, potentially mediated via calcitonin gene-related peptide (CGRP) receptors [14]. Therefore, investigating the specific mechanisms of action between calcitonin and sepsis is crucial for developing improved therapeutic strategies.

CD3D, also known as CD3 delta chain, is a protein encoded by the *CD3D* gene and constitutes an essential component of the CD3 complex [15]. As a key player in T cell growth and T cell receptor (TCR) signaling, this complex is essential for signal transmission in T cells. Deficiency or dysfunction of *CD3D* impairs T cell function and disrupts immune homeostasis, thereby contributing to various autoimmune disorders and immunodeficiencies [16]. In the context of sepsis, *CD3D* has been recognized as a potential marker of immune dysfunction and disease severity [17]. Yang *et al.* [18] conducted a bioinformatics analysis investigating the association between *CD3D*, *CD247*, and septic shock, demonstrating that reduced expression of both *CD3D* and *CD247* correlated with poor prognosis. Nevertheless, the relationship between *CD3D*, sepsis, and calcitonin therapy is not yet well defined, underscoring the necessity of additional research to determine its value as a prognostic biomarker or therapeutic target in sepsis management.

Although *CD3D* has been recognized by recent transcriptome analysis as a possible immune-related biomarker in sepsis, its precise function in pulmonary endothelium damage remains unclear. This work combined bioinformatics analyses with experimental approaches to explore the role of *CD3D* in sepsis-induced ALI, focusing on its participation in oxidative stress, inflammatory, and apoptotic pathways in human pulmonary microvascular endothelial cells (hPMECs). In several inflammatory illness models, calcitonin has shown cytoprotective and anti-inflammatory qualities. Nevertheless, whether calcitonin contributes to the preservation of pulmonary microvascular endothelial integrity during sepsis, particularly through modulation of immune signaling pathways, remains unclear. Therefore, this research aims to comprehensively examine the function of *CD3D* and the possibility of calcitonin as a treatment for sepsis-induced ALI.

2. Materials and Methods

2.1 Dataset Sources and Differential Expression Analysis

The Gene Expression Omnibus (GEO, https://www.ncbi.nlm.nih.gov/gds/) provided the sepsis-related dataset GSE89376. A total of 12 sepsis and 12 control samples were analyzed. Differential expression was assessed using the "limma" package in R (version 4.0; R Foundation for Statistical Computing, Vienna, Austria), with thresholds set at FC >1.3 for upregulation, FC <0.7 for downregulation, and $p < 0.05$ for statistical significance [19]. To further identify hub genes, the dataset GSE67652 was also obtained from the GEO database for validation. This dataset included samples from an additional 12 septic patients and 12 healthy controls.

2.2 Functional Annotation of Differentially Expressed Genes (DEGs)

DEGs were subjected to functional enrichment employing the Database for Annotation, Visualization, and Integrated Discovery (DAVID; https://davidbioinformatics.nih.gov/summary.jsp). Gene ontology, along with Kyoto Encyclopedia of Genes and Genomes (KEGG) pathways, was identified and visualized.

2.3 Protein-Protein Interaction (PPI) Network Construction and Expression Profiling of Overlapping Genes

To explore interactions among DEGs, a PPI network was established using the STRING platform (https://string-db.org/). Key modules were identified in Cytoscape (version 3.8.1; Cytoscape Consortium San Diego, CA, USA) via CytoHubba with Degree, Maximum Neighborhood Component (MNC), and Maximal Clique Centrality (MCC) algorithms. Overlapping genes across modules were identified through the Venn analysis tool (https://bioinformatics.psb.ugent.be/webtools/Venn/). Their expression patterns were subsequently validated in the GSE89376 and GSE67652 datasets by comparing septic and control samples. Data analysis and visualization were performed with Sangerbox (http://vip.sangerbox.com/home.html).

2.4 Study Population, Sample Collection, and Serum Cytokine Quantification in Sepsis and ALI

A total of nine participants were enrolled in this investigation, including three patients with sepsis-induced ALI, three patients with sepsis without pulmonary involvement, and three non-septic control patients without pulmonary inflammation. Sepsis patients were admitted to the Department of Intensive Care Medicine. In contrast, control patients were recruited from the Department of Hepatobiliary Surgery, the Third Affiliated Hospital of Naval Military Medical University. All participants were age- and gender-matched. Sepsis was identified using the Sepsis-3 criteria, which include life-threatening organ dysfunction and a Sequential Organ Failure Assessment (SOFA) score rise of ≥ 2

caused by a dysregulated host response to infection. Control participants were hospitalized for non-infectious hepatobiliary conditions and showed no evidence of systemic disease, sepsis, or lung injury at the time of sampling. All participants and their legal guardians provided written informed consent. The study protocol was evaluated and approved by Academic Committee of the Third Affiliated Hospital of Naval Medical University (Approval Number: KY2024081), and it followed the Declaration of Helsinki. Since the patient's condition is fixed, random allocation is not possible. All subjects had peripheral venous blood drawn within 24 hours of either elective admission (for controls) or intensive care unit (ICU) admission (for septic patients). After centrifugation of blood specimens (3000 rpm, 10 min, 4 °C), serum was collected, portioned, and maintained at –80 °C pending analysis. Serum concentrations of CD3D, MyD88, high-mobility group box 1 (HMGB1), NLR family pyrin domain containing 3 (NLRP3), and phosphorylation of nuclear factor-κB (p-NF-κB) were detected by human enzyme-linked immunosorbent assay (ELISA) kits. Specifically, the human CD3D ELISA kit (Cat. no. XY-EH1234) was purchased from Xinyu Biotechnology Co., Ltd. (Shanghai, China). ELISA kits for HMGB1 (Cat. no. JL13693-48T), p-NF-κB (Cat. no. JL42948-48T), and NLRP3 (Cat. no. JL10272-48T) were obtained from Jianglai Biological Technology (Shanghai, China). The MyD88 ELISA kit (Cat. no. ab171341) was sourced from Abcam (Shanghai, China). The manufacturers' protocols applied to all assays. Utilizing a microplate reader (Cat. no. DNM-9606; Perlong, Beijing, China), absorbance was measured at 450 nm.

2.5 Culture Conditions and Treatment Protocols

hPMECs (Cat. no. CP-H001, Procell, Wuhan, China) were cultured in complete hPMEC medium (Cat. no. CM-H001, Procell, Wuhan, China) under standard conditions of 37 °C with 5% CO_2. According to the supplier's quality control statement, hPMECs were authenticated by CD31 immunofluorescence and tested to be over 90% pure. Additionally, the supplier confirmed that the cells were free from human immunodeficiency virus (HIV)-1, hepatitis B virus (HBV), hepatitis C virus (HCV), Mycoplasma, bacteria, fungi, and yeast contamination. To establish a sepsis-induced ALI model, cells were exposed to LPS (10 µg/mL; Cat. no. L8880, Solarbio, Beijing, China) for 24 h. For evaluating the protective role of calcitonin, LPS-treated hPMECs were further incubated with calcitonin (Cat. no. T3535, Sigma-Aldrich, St. Louis, MO, USA) at concentrations of 1, 5, and 10 nM for 24 h.

2.6 Cell Transfection

After being seeded at a density of 2×10^5 cells per well in 24-well plates, hPMECs were cultivated in full growth media for the whole night until they attained a confluency of around 70–80%. As directed by the manufacturer, Lipofectamine 2000 transfection reagent (Invitrogen, Carlsbad, CA, USA) was used for transfection. In particular, hPMECs were transfected with either *CD3D*-targeting small interfering RNAs (siRNAs; si-*CD3D*-1 and si-*CD3D*-2) or a negative control siRNA (si-NC). After 48 hours of transfection, cells were harvested for further experimentation.

2.7 Quantitative Real-Time Polymerase Chain Reaction (qRT-PCR)

RNA purity and concentration were determined with a NanoDrop spectrophotometer (Thermo Fisher Scientific, Shanghai, China). First-strand cDNA was synthesized from 1 µg of RNA using the PrimeScript RT Kit (Takara, Shiga, Japan). qRT-PCR was performed on a StepOnePlus Real-Time PCR System (Applied Biosystems, Shanghai, China) using SYBR Green PCR Master Mix (Cat. no. 4309155; Thermo Fisher Scientific, Waltham, MA, USA). All reactions were performed in triplicate. Relative gene expression levels were calculated using the $2^{-\Delta\Delta Ct}$ method, with glyceraldehyde-3-phosphate dehydrogenase (GAPDH) serving as the internal control. Primer sequences are provided in Table 1.

2.8 Western Blotting (WB)

hPMEC proteins were isolated using radioimmunoprecipitation assay (RIPA) buffer (Cat. no. 89900; Thermo Fisher Scientific, Waltham, MA, USA) supplemented with protease and phosphatase inhibitors. Protein levels were measured using a bicinchoninic acid (BCA) assay (Cat. no. P0011; Beyotime, Shanghai, China). Equal quantities of protein were subjected to sodium dodecyl sulfate polyacrylamide gel electrophoresis (SDS-PAGE) and subsequently blotted onto poly-vinylidene difluoride (PVDF) membranes (Cat. no. FFP39; Beyotime, Shanghai, China). The membranes were blocked and subsequently incubated with primary antibodies against CD3D (1:1000, ab109531), p21 (1:2000, ab109520), Cyclin D1 (1:1000, ab109531), cyclin dependent kinase 2 (CDK2) (1:1000, ab32147), cyclooxygenase-2 (COX-2) (1:2000, ab179800), inducible Nitric Oxide Synthase (iNOS) (1:2000, ab178945), HMGB1 (1:1000, ab92310), MyD88 (1:1000, ab133739), p-NF-κB (1:1000, ab207297), NF-κB (1:1000, ab283716), NLRP3 (1:1000, ab263899), Bcl-2 (1:2000, ab182858), Bax (1:2000, ab32503), and Caspase-3 (1:5000, ab32351), with GAPDH (1:2500, ab9485) serving as a loading control. All antibodies were purchased from Abcam (Shanghai, China). After secondary antibody incubation with Goat Anti-Rabbit IgG H&L (horseradish peroxidase (HRP), 1:10,000, ab6721), proteins were visualized by enhanced chemiluminescence (ECL) (Cat. no. P0018FS; Beyotime, Shanghai, China), and band intensities were quantified through ImageJ (version 1.54; National Institutes of Health, Bethesda, MD, USA) analysis.

Table 1. Primer sequences for qRT-PCR.

Target	Direction	Sequence (5′-3′)
CD3D	Forward	AGACTGGACCTGGGAAAACG
CD3D	Reverse	AGACTCCCAAAGCAAGGAGC
p21	Forward	AGTCAGTTCCTTGTGGAGCC
p21	Reverse	CATTAGCGCATCACAGTCGC
CCND1	Forward	GATGCCAACCTCCTCAACGA
CCND1	Reverse	ACTTCTGTTCCTCGCAGACC
CDK2	Forward	GACACGCTGCTGGATGTCA
CDK2	Reverse	CTGGAGCAGCTGGAACAGAT
iNOS	Forward	AATGTGGAGAAAGCCCCCTG
iNOS	Reverse	TGCATCCAGCTTGACCAGAG
COX-2	Forward	GGCCATGGGGTGGACTTAAA
COX-2	Reverse	ACCGTAGATGCTCAGGGACT
HMGB1	Forward	TCTCAGGGCCAAACCGATAG
HMGB1	Reverse	TCGTGCACCGAAAGTTTCAA
MyD88	Forward	ACTTGGAGATCCGGCAACTG
MyD88	Reverse	ATCCGGCGGCACCAATG
NLRP3	Forward	GCTGGCATCTGGGGAAACCT
NLRP3	Reverse	CAAGTCCACATCCTCCAGGTC
Bax	Forward	TGATGGACGGGTCCGGG
Bax	Reverse	TGAGACACTCGCTCAGCTTC
Bcl-2	Forward	AACCTTTCAGCATCACAGAGGAAGT
Bcl-2	Reverse	AGGGGGTGTCTTCAATCACG
CASP3	Forward	TGTGAGGCGGTTGTAGAAGAGT
CASP3	Reverse	CTTTATTAACGAAAACCAGAGCGCC
GAPDH	Forward	AATGGGCAGCCGTTAGGAAA
GAPDH	Reverse	GCGCCCAATACGACCAAATC

qRT-PCR, quantitative real-time polymerase chain reaction; *CD3D*, CD3 delta subunit of T-cell receptor complex; *p21*, cyclin-dependent kinase inhibitor 1A (*CDKN1A*); *CCND1*, cyclin D1; *CDK2*, cyclin dependent kinase 2; *iNOS*, inducible Nitric Oxide Synthase; *COX-2*, cyclooxygenase-2; *HMGB1*, high-mobility group box 1; *MyD88*, myeloid differentiation primary response gene 88; *NLRP3*, NLR family pyrin domain containing 3; *Bax*, Bcl-2 associated X; *Bcl-2*, B-cell lymphoma-2; *CASP3*, caspase-3; *GAPDH*, glyceraldehyde-3-phosphate dehydrogenase.

2.9 Assay for Cell Counting Kit-8 (CCK-8)

Cell proliferation and viability were determined by CCK-8 assay (Cat. no. C0042; Beyotime, China). Briefly, hPMECs were seeded in 96-well plates at a density of 5×10^3 cells per well with 100 µL of complete culture medium. Untreated or treated cells were incubated for 24, 36, 48, 72, and 96 hours. CCK-8 solution (10 µL) was added at each time point, and optical density at 450 nm was measured after 2 h using a microplate reader (Model DNM-9602; Perlong, Beijing, China).

2.10 Flow Cytometry

Apoptosis and cell-cycle profiles of hPMECs were determined by flow cytometry. After 24 h culture in 24-well plates (1×10^5 cells/well), cells for apoptosis assays were digested with trypsin-ethylenediaminetetraacetic acid (EDTA), rinsed in phosphate-buffered saline (PBS), and incubated with Annexin V-FITC (5 µL) and PI (5 µL) in the dark for 15 min. Stained cells were examined on a flow cytometer (ACEA Biosciences, China), and results were analyzed with FlowJo (Version 10.8.1, FlowJo, LLC, Ashland, OR, USA). To analyze the cell cycle, cells were fixed with 75% ethanol (4 h, 4 °C), stained with PI (50 µg/mL) plus RNase A (10 mg/L) for 1 h at 37 °C, and subjected to flow cytometry.

2.11 Enzyme-Linked Immunosorbent Assay (ELISA)

Tumor necrosis factor (TNF)-α (Cat. no. MM-0122H2), interleukin (IL)-6 (Cat. no. MM-0049H2), and IL-1β (Cat. no. MM-0181H2) levels in culture supernatants were measured using ELISA kits (Meimian, Jiangsu, China) according to the manufacturer's instructions. After adding samples and standards to capture antibody-coated wells, plates were incubated for 2 h at 37 °C. Detection was performed using HRP-conjugated antibodies and 3,3′,5,5-tetramethylbenzidine (TMB) substrate, and absorbance was measured at 450 nm with a microplate reader (Model DNM-9602; Perlong, Beijing, China). The concentrations of cytokines were measured using standard curves as a guide.

2.12 Quantification of Cellular Metabolism and Oxidative Stress Markers in hPMECs

To determine cellular metabolic and oxidative stress markers, hPMECs were cultured in 24-well plates (1×10^5 cells/well), washed with PBS, and lysed. After centrifugation at 10,000 $\times$g for 5 min at 4 °C, supernatants were collected. Biochemical parameters were analyzed with commercial kits (Nanjing Jiancheng Bioengineering Institute, China), including lactate dehydrogenase (LDH, Cat. no. A020-1-2) activity (440 nm), malondialdehyde (MDA, Cat. no. A003-4-1) content (532 nm), superoxide dismutase (SOD, Cat. no. A001-3-2) activity (450 nm), and glutathione (GSH, Cat. no. A006-1-1) levels (420 nm).

2.13 Data Analysis and Statistics

At least three independent experiments were carried out for each dataset. Statistical evaluation was conducted in R. Differences between the two groups were determined using Student's *t*-test. In contrast, multiple-group comparisons were analyzed by one-way analysis of variance (ANOVA) with Tukey's *post-hoc* test. Data are shown as mean $\pm$ SD, with statistical significance defined at $p < 0.05$.

3. Results

3.1 Analysis of DEGs and Functional Enrichment in the GSE89376 Dataset

From the GSE89376 dataset, 182 genes were found to be upregulated and 178 downregulated (Fig. 1A). DEGs were significantly enriched in biological processes (BP)-

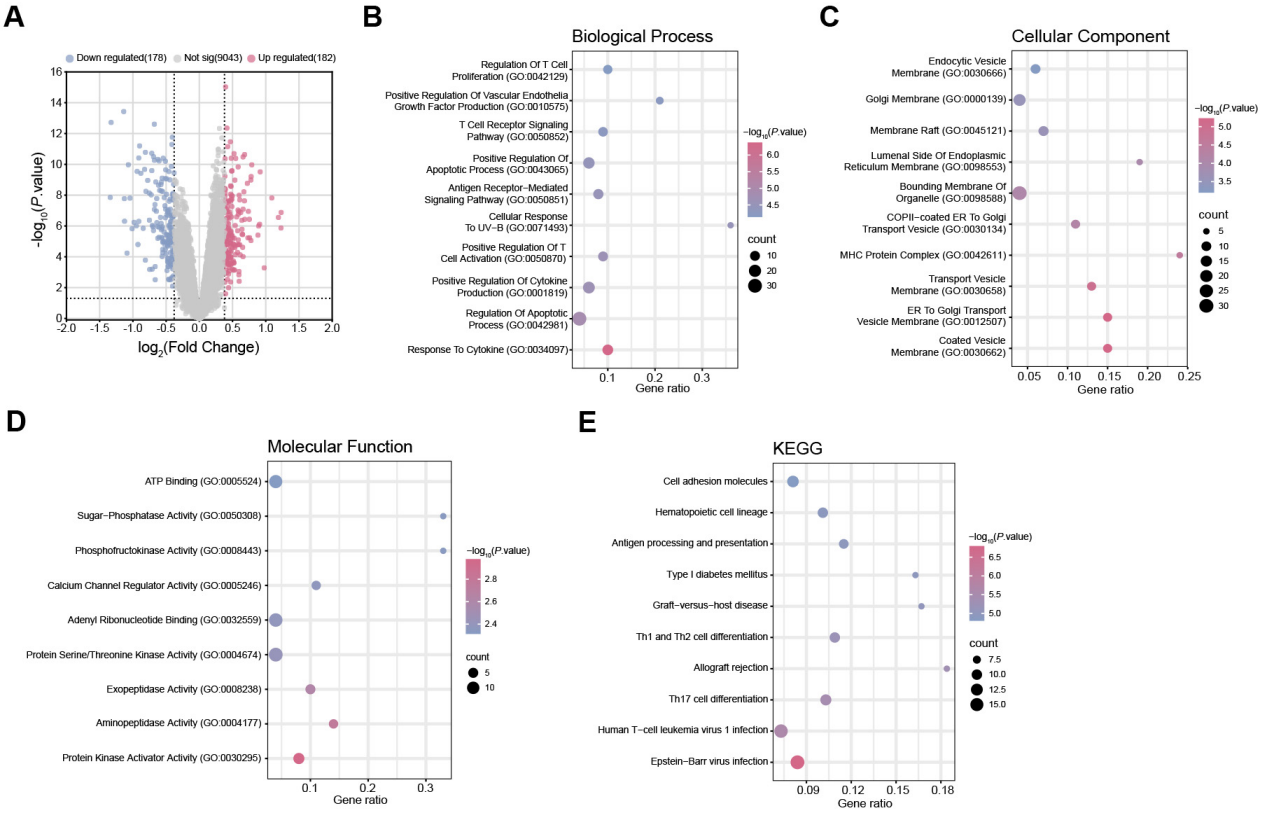

Fig. 1. Differential gene expression and functional enrichment analysis. (A) Volcano plot displaying identified DEGs from the GSE89376 dataset. Each point represents an individual gene. Up-regulated DEGs are depicted in pink, and down-regulated DEGs are depicted in blue. (B) GO enrichment analysis of BP terms associated with DEGs. The x-axis represents the GeneRatio, and the y-axis indicates the enriched terms. The size of the dots corresponds to the number of genes, and the color reflects the adjusted *p* value. (C) GO enrichment analysis of CC terms of DEGs. (D) GO enrichment analysis of MF terms of DEGs. (E) KEGG enrichment analysis predicted the pathways of DEGs involvement. DEGs, Differential Expressed Genes; GO, Gene Ontology; BP, Biological process; CC, Cell component; MF, Molecular function; KEGG, Kyoto Encyclopedia of Genes and Genomes.

related GO terms, mainly involving "Positive regulation of apoptotic process", "Regulation of T cell proliferation", and "Positive regulation of vascular endothelial growth factor production" (Fig. 1B). For cellular components (CC), enrichment was observed in "Coated vesicle membrane", "ER-to-Golgi transport vesicle membrane", and "Endocytic vesicle membrane" (Fig. 1C). Regarding molecular function (MF), DEGs were enriched in "Protein kinase activator activity", "Exopeptidase activity", and "Calcium channel regulator activity" (Fig. 1D). KEGG pathway analysis further indicated enrichment in "Human T-cell leukemia virus 1 infection", "Cell adhesion molecules", as well as "Hematopoietic cell lineage" (Fig. 1E).

3.2 Screening and Validation of Candidate Genes Associated With Sepsis

Candidate genes associated with sepsis were identified using PPI network analysis. Three topological algorithms (MNC, MCC, and Degree) were applied to screen for hub genes, and the top 10 genes ranked by each algorithm were selected for comparison (Fig. 2A–C). Venn diagram analysis revealed four overlapping genes across all three algorithms: *CR7*, *CD247*, *CD3D*, and *CD69* (Fig. 2D). Expression profiling using the GSE89376 dataset showed significant upregulation of all four genes in sepsis patients compared with controls (Fig. 2E). Validation in an independent dataset (GSE67652) confirmed their consistently elevated expression (Fig. 2F). In the GSE89376 dataset, the Cohen's d for *CD3D* was 3.36, with a 95% confidence interval (CI) of 0.43–0.71 ($p < 0.0001$); In the GSE67652 dataset, the Cohen's d for *CD3D* was 2.10, with a 95% CI of 0.26–0.61 ($p < 0.0001$). These results indicate that *CD3D* exhibited a significant effect size in both datasets, suggesting it may play an essential role in related biological processes. Notably, *CD3D* displayed the most important differential expression in both datasets, making it a candidate for further functional studies.

3.3 Elevated Serum Levels of CD3D, HMGB1, p-NF-κB, MyD88, and NLRP3 in Sepsis and Sepsis-Induced ALI

HMGB1 has been reported to activate NF-κB via a MyD88-dependent pathway, thereby providing transcrip-

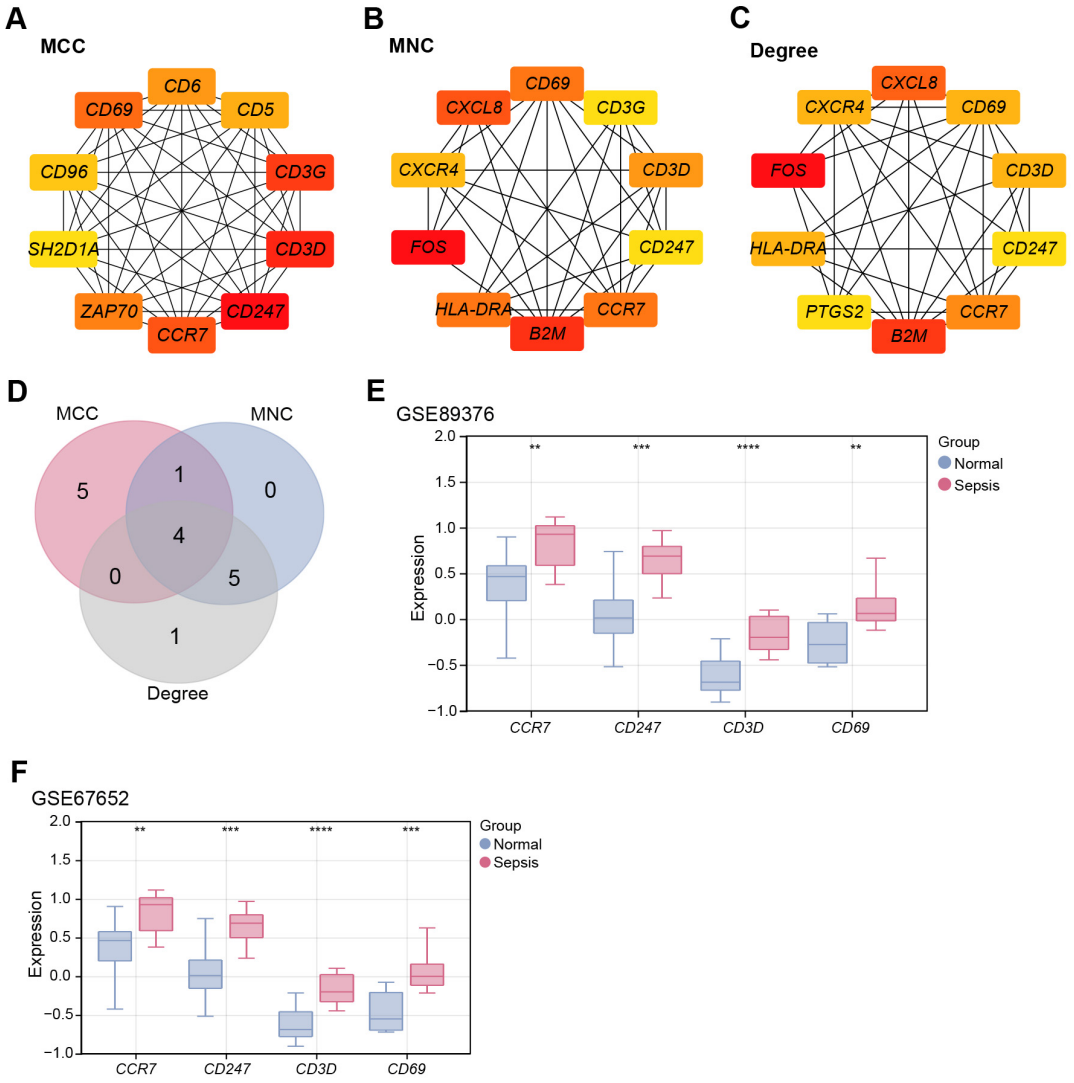

Fig. 2. Identification of *CD3D* as a key hub gene in sepsis pathogenesis. (A) PPI network constructed using the MCC algorithm, showing the top ten highly interconnected genes (10 nodes and 45 edges). (B) PPI network constructed using the MNC algorithm, displaying the top ten hub genes (10 nodes and 34 edges). (C) PPI network constructed using the Degree algorithm, highlighting the top ten hub genes (10 nodes and 33 edges). (D) Venn diagram of the top ten genes identified by the MCC, MNC, and Degree algorithms, with four overlapping hub genes obtained. (E) Box plots of the expression levels of overlapping hub genes (*CCR7*, *CD247*, *CD3D*, and *CD69*) in sepsis and normal samples from the GSE89376 dataset. (F) Validation of the expression of overlapping hub genes (*CCR7*, *CD247*, *CD3D*, and *CD69*) in the GSE67652 dataset. $^{**}p < 0.01$ or $^{***}p < 0.001$ or $^{****}p < 0.0001$ vs. Normal group. PPI, Protein-Protein Interaction; MCC, Maximal Clique Centrality; MNC, Maximum Neighborhood Component.

tional priming for NLRP3 inflammasome expression [20]. A previous study has highlighted the critical role of NF-κB signaling in sepsis [21]. To investigate immune-inflammatory signaling changes in sepsis and sepsis-induced ALI, serum levels of CD3D, HMGB1, MyD88, NF-κB, and NLRP3 were measured by ELISA. Compared with the healthy controls, sepsis patients exhibited significantly higher concentrations of CD3D (Cohen's d = 2.63, 95% CI: 0.44–4.8), HMGB1 (Cohen's d = 4.48, 95% CI: 1.48–7.48), MyD88 (Cohen's d = 3.66, 95% CI: 1.04–6.28), NF-κB (Cohen's d = 4.86, 95% CI: 1.68–8.05), and NLRP3 (Cohen's d = 4.69, 95% CI: 1.59–7.79). Moreover, serum levels of CD3D (Cohen's d = 2.20, 95% CI: 0.17–4.22), HMGB1 (Cohen's d = 5.55, 95% CI: 2.02–9.07), MyD88 (Cohen's d = 3.04, 95% CI: 0.69–5.38), NF-κB (Cohen's d = 5.13, 95% CI: 1.81–8.44), NLRP3 (Cohen's d = 10.98, 95% CI: 4.57–17.40) were further elevated in sepsis patients with ALI compared to those without pulmonary involvement (Fig. 3A–E). Collectively, these findings suggest that HMGB1 promotes NLRP3 inflammasome activation via a MyD88-dependent NF-κB pathway, thereby contributing to inflammatory injury in sepsis and sepsis-associated ALI.

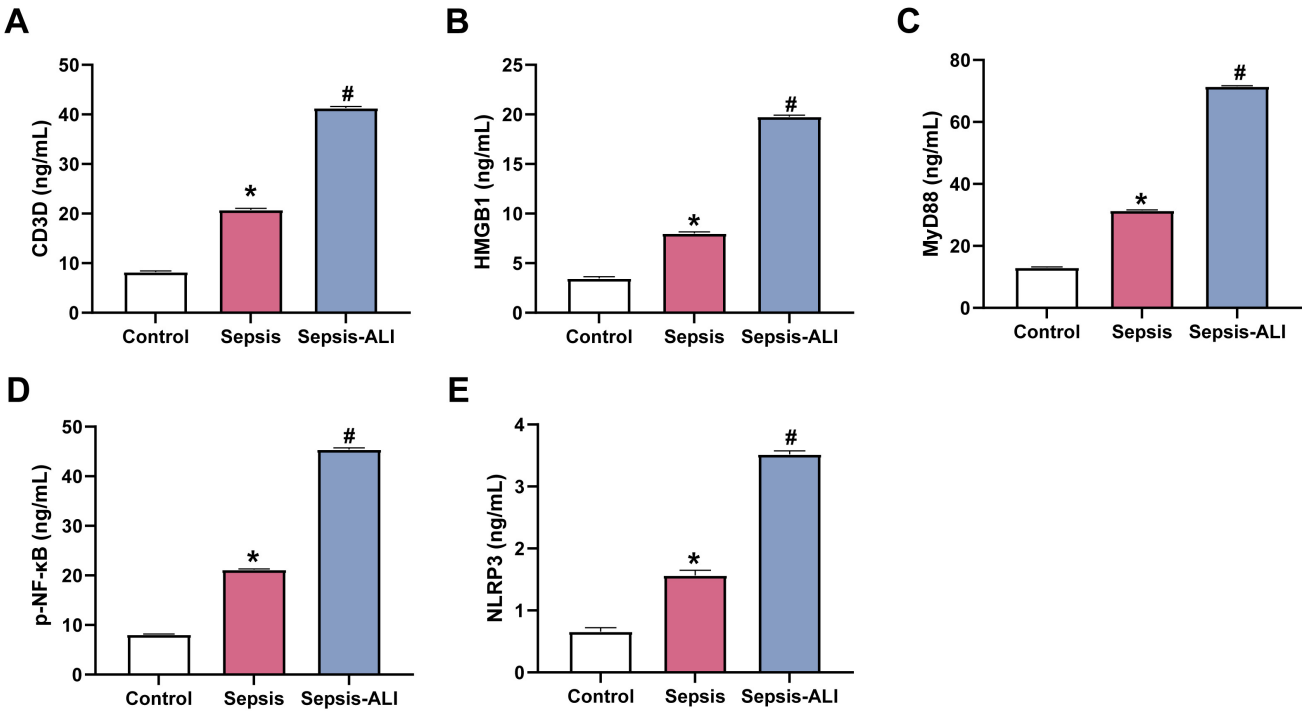

Fig. 3. Sepsis and sepsis-induced ALI are associated with elevated serum levels of CD3D, HMGB1, MyD88, p-NF-κB, and NLRP3. (A) Serum CD3D concentrations were measured by ELISA in the control, patients with sepsis (Sepsis), and patients with sepsis-associated acute lung injury (Sepsis-ALI). (B) Serum HMGB1 concentrations were measured by ELISA in the control, Spesis, and Sepsis-ALI groups. (C) Serum MyD88 concentrations were measured by ELISA in the control, Spesis, and Sepsis-ALI groups. (D) Serum p-NF-κB concentrations were measured by ELISA in the control, Spesis, and Sepsis-ALI groups. (E) Serum NLRP3 concentrations were measured by ELISA in the control, Spesis, and Sepsis-ALI groups. Each assay was performed in triplicate to ensure accuracy and reproducibility. Statistical significance was determined by comparing the mean values of each group. $*p < 0.05$ vs. Control group, $^{\#}p < 0.05$ vs. Sepsis group. ALI, acute lung injury; HMGB1, high-mobility group box 1; p-NF-κB, phosphorylation of nuclear factor-κB; NLRP3, NLR family pyrin domain containing 3; ELISA, enzyme-linked immunosorbent assay.

3.4 CD3D Knockdown Attenuates LPS-Induced Inflammatory Response and Proliferation Inhibition in hPMECs

The knockdown efficiency of two *CD3D*-targeting siRNAs in hPMECs was assessed by qRT-PCR and WB. Both siRNAs effectively reduced *CD3D* expression, with si-*CD3D*-2 showing the most substantial effect and therefore used for subsequent experiments (Fig. 4A–C). To mimic the septic inflammatory microenvironment, hPMECs were stimulated with LPS. LPS significantly increased *CD3D* expression compared with controls, whereas *CD3D* knockdown suppressed this induction (Fig. 4D–F). ELISA analysis revealed that LPS stimulation significantly promoted the secretion of TNF-α, IL-6, and IL-1β, whereas *CD3D* knockdown reduced these pro-inflammatory effects (Fig. 4G). CCK-8 assays revealed that LPS inhibited hPMEC proliferation, whereas *CD3D* knockdown partially restored proliferation (Fig. 4H). These results indicate that *CD3D* knockdown mitigates LPS-induced inflammatory cytokine production and inhibition of proliferation in hPMECs.

3.5 CD3D Knockdown Reverses LPS-Induced G1 Cell Cycle Arrest in hPMECs

To investigate the effect of *CD3D* knockdown on cell cycle progression, flow cytometry was performed. LPS exposure reduced the S-phase population and increased the proportion of cells in the G1 phase, indicating G1 arrest. *CD3D* knockdown partially reversed this effect, reducing G1 accumulation and increasing the S-phase fraction (Fig. 5A). Consistently, qRT-PCR showed that LPS treatment upregulated *p21* expression while downregulating *Cyclin D1* and *CDK2*. These transcriptional changes were reversed by *CD3D* knockdown and further confirmed at the protein level by WB (Fig. 5B–D). These findings suggest that *CD3D* silencing alleviates LPS-induced G1 arrest by modulating cell cycle regulators.

3.6 CD3D Silencing Mitigates LPS-Induced Oxidative Stress in hPMECs

To further evaluate the role of *CD3D* in sepsis-induced ALI, particularly in relation to oxidative stress, ELISA was used to measure LDH, MDA, SOD, and GSH levels. LPS stimulation significantly increased LDH and MDA, while

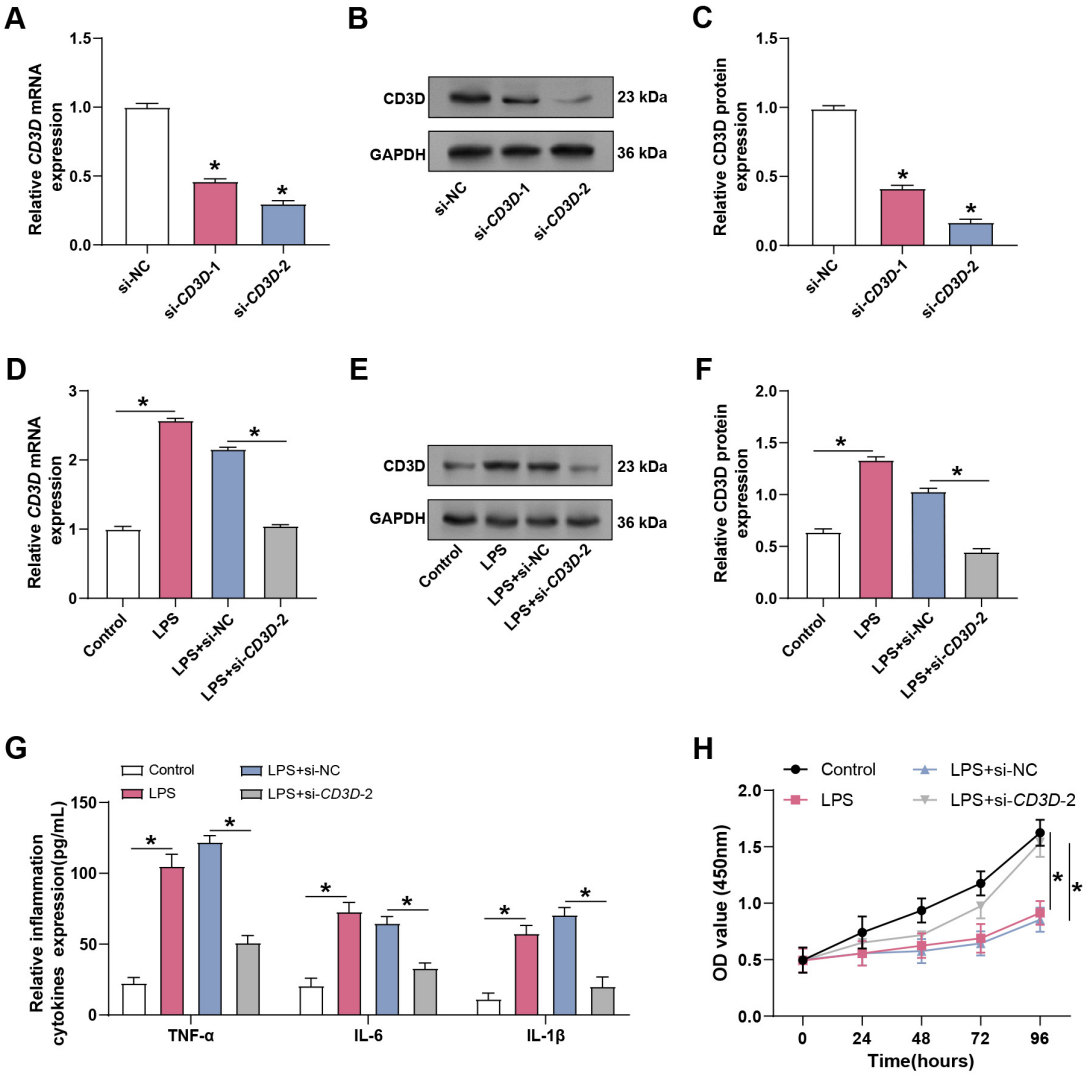

Fig. 4. Knockdown of *CD3D* alleviates LPS-induced ALI in hPMECs. (A) qRT-PCR analysis of *CD3D* mRNA expression in hPMECs following transfection with *CD3D*-specific siRNA. *$p < 0.05$ vs. si-NC group. (B) WB analysis of CD3D protein expression after siRNA transfection in hPMECs. (C) Quantification of CD3D protein levels following knockdown. *$p < 0.05$ vs. si-NC group. (D) qRT-PCR analysis of *CD3D* mRNA levels in hPMECs treated with LPS alone or in combination with *CD3D* knockdown. (E) WB analysis of CD3D protein expression in LPS-treated hPMECs with or without CD3D knockdown. (F) Quantification of CD3D protein levels under LPS stimulation with or without CD3D knockdown, normalized with GAPDH. (G) ELISA-based quantification of TNF-α, IL-6, and IL-1β levels in the supernatants of hPMECs following LPS stimulation with or without *CD3D* knockdown. (H) Cell viability assessment by CCK-8 assay in hPMECs exposed to LPS with or without *CD3D* knockdown. hPMECs, human pulmonary microvascular endothelial cells; qRT-PCR, Quantitative Real-Time Polymerase Chain Reaction; WB, Western Blotting; CCK-8, Cell Counting Kit-8; LPS, Lipopolysaccharide. Each assay was performed in triplicate to ensure accuracy and reproducibility. Statistical significance was determined by comparing the mean values of each group. *$p < 0.05$.

decreasing SOD and GSH, indicating enhanced oxidative stress and damage. *CD3D* knockdown reversed these effects by lowering LDH and MDA and restoring GSH and SOD (Fig. 6A–D). In addition, LPS strongly upregulated *COX-2* and *iNOS*, two key inflammatory mediators, at both mRNA and protein levels, whereas *CD3D* knockdown suppressed this induction (Fig. 6E–I). These results suggest that *CD3D* plays a role in LPS-induced oxidative stress and inflammatory responses in hPMECs.

3.7 Calcitonin Alleviates LPS-Induced Inflammatory Injury in hPMECs in a Dose-Dependent Manner

Calcitonin, secreted by thyroid parafollicular C cells, is known to reduce serum calcium levels [22]. To explore its protective role, hPMECs were treated with calcitonin at concentrations of 1, 5, and 10 nM under LPS stimulation. Calcitonin alone did not significantly alter cell viability. However, LPS markedly reduced viability, which was restored by calcitonin in a dose-dependent

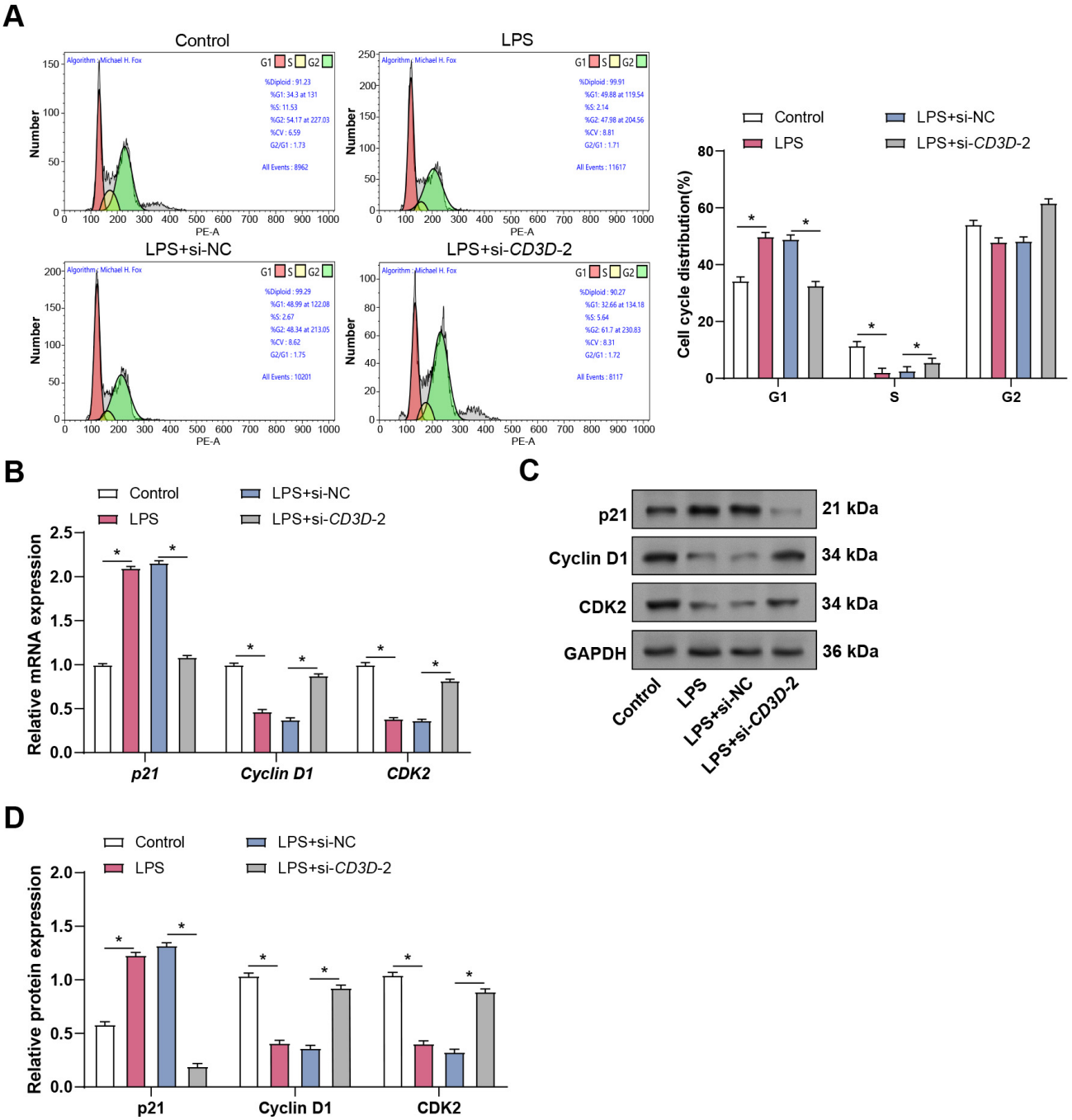

Fig. 5. Effect of *CD3D* knockdown on sepsis-related LPS-induced hPMECs cell cycle. (A) Flow cytometry analysis depicts the cell cycle distribution in hPMECs stimulated with LPS alone or in combination with *CD3D* knockdown. (B) qRT-PCR analysis of *p21*, *Cyclin D1*, and *CDK2* mRNA expression in hPMECs treated with 10 µg/mL LPS alone or in combination with *CD3D* knockdown. (C) WB analysis of p21, Cyclin D1, and CDK2 protein levels in hPMECs following 24-hour LPS stimulation with or without *CD3D* knockdown. (D) Quantification of p21, Cyclin D1, and CDK2 protein expression levels based on WB results. Each assay was performed in triplicate to ensure accuracy and reproducibility. Statistical significance was determined by comparing the mean values of each group. *$p < 0.05$.

manner (Fig. 7A). WB further revealed that calcitonin had no significant effect on CD3D protein expression in control cells; however, in LPS-stimulated hPMECs, calcitonin suppressed CD3D expression in a concentration-dependent manner (Fig. 7B,C). Flow cytometry analysis further showed that calcitonin attenuated LPS-induced apoptosis in a concentration-dependent manner (Fig. 7D,E). Consistently, ELISA results indicated that calcitonin suppressed LPS-induced secretion of TNF-α, IL-6, and IL-1β, while not affecting their basal levels (Fig. 7F–H).

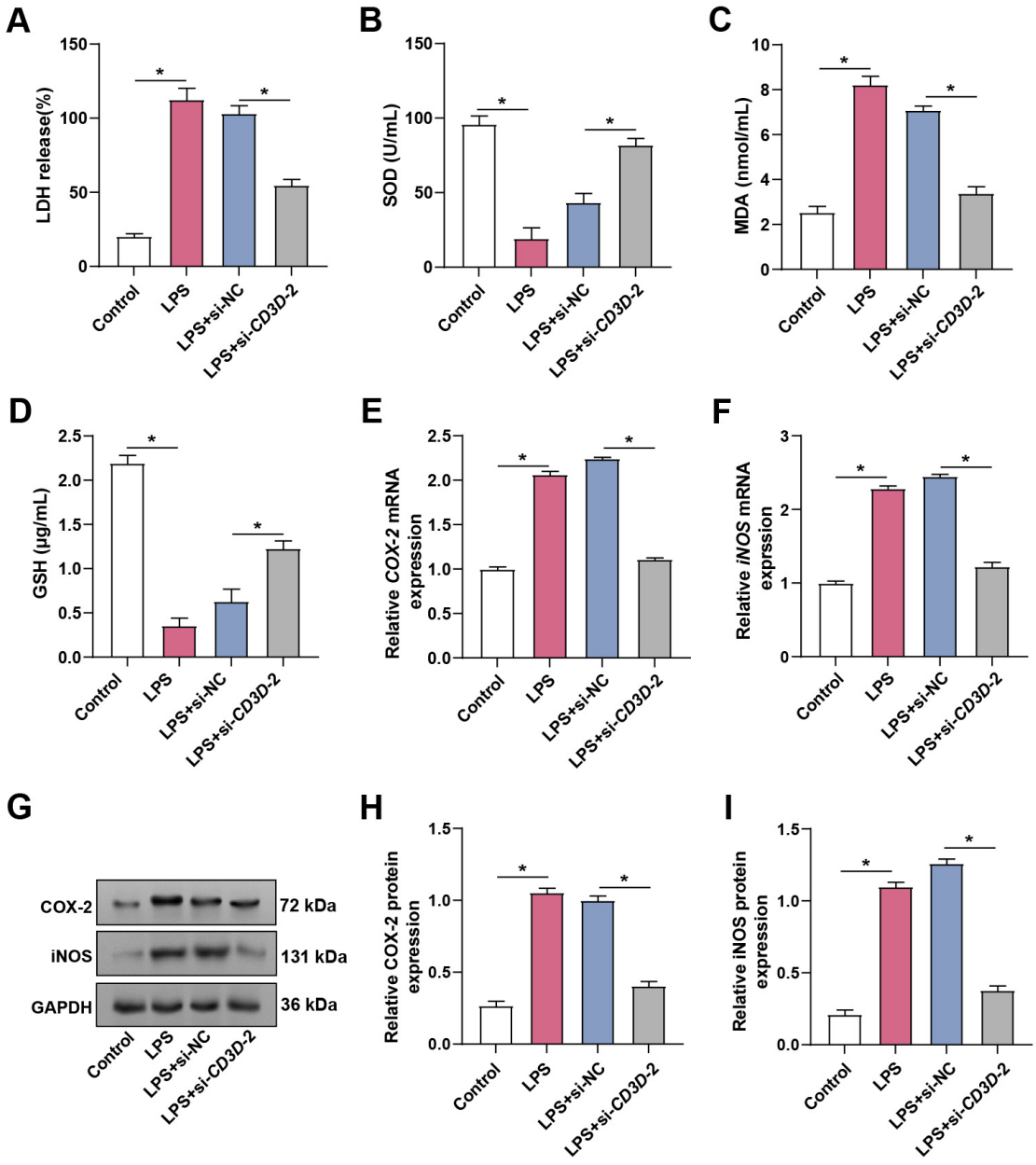

Fig. 6. Effects of *CD3D* knockdown on oxidative stress and inflammatory markers in LPS-treated hPMECs. (A) LDH release in hPMECs after treatment with 10 μg/mL LPS alone or in combination with *CD3D* knockdown for 24 hours. (B) SOD activity in hPMECs under the indicated treatments. (C) MDA levels measured in hPMECs under the indicated treatments. (D) GSH levels in hPMECs under the indicated treatments. (E) qRT-PCR analysis of *COX-2* mRNA expression in hPMECs treated with LPS alone or combined with *CD3D* knockdown. (F) qRT-PCR analysis of *iNOS* mRNA expression in hPMECs under the same conditions. (G) Representative WB images showing COX-2 and iNOS protein levels in hPMECs stimulated with LPS with or without *CD3D* knockdown. GAPDH served as the loading control. (H) Quantification of COX-2 protein expression from WB analysis. (I) Quantification of iNOS protein expression from WB analysis. LDH, Lactate Dehydrogenase; SOD, Superoxide Dismutase; MDA, Malondialdehyde; GSH, Glutathione. Each assay was performed in triplicate to ensure accuracy and reproducibility. Statistical significance was determined by comparing the mean values of each group. *$p < 0.05$.

3.8 Calcitonin Attenuates LPS-Induced Oxidative Stress in hPMECs

To evaluate the effects of calcitonin on oxidative stress, ELISA was used to measure SOD, MDA, and GSH levels. LPS stimulation significantly increased MDA, while decreasing SOD and GSH, indicating oxidative stress and injury. Co-treatment with calcitonin reversed these changes in a dose-dependent manner, reducing MDA levels and restoring SOD and GSH activity (Fig. 8A–C).

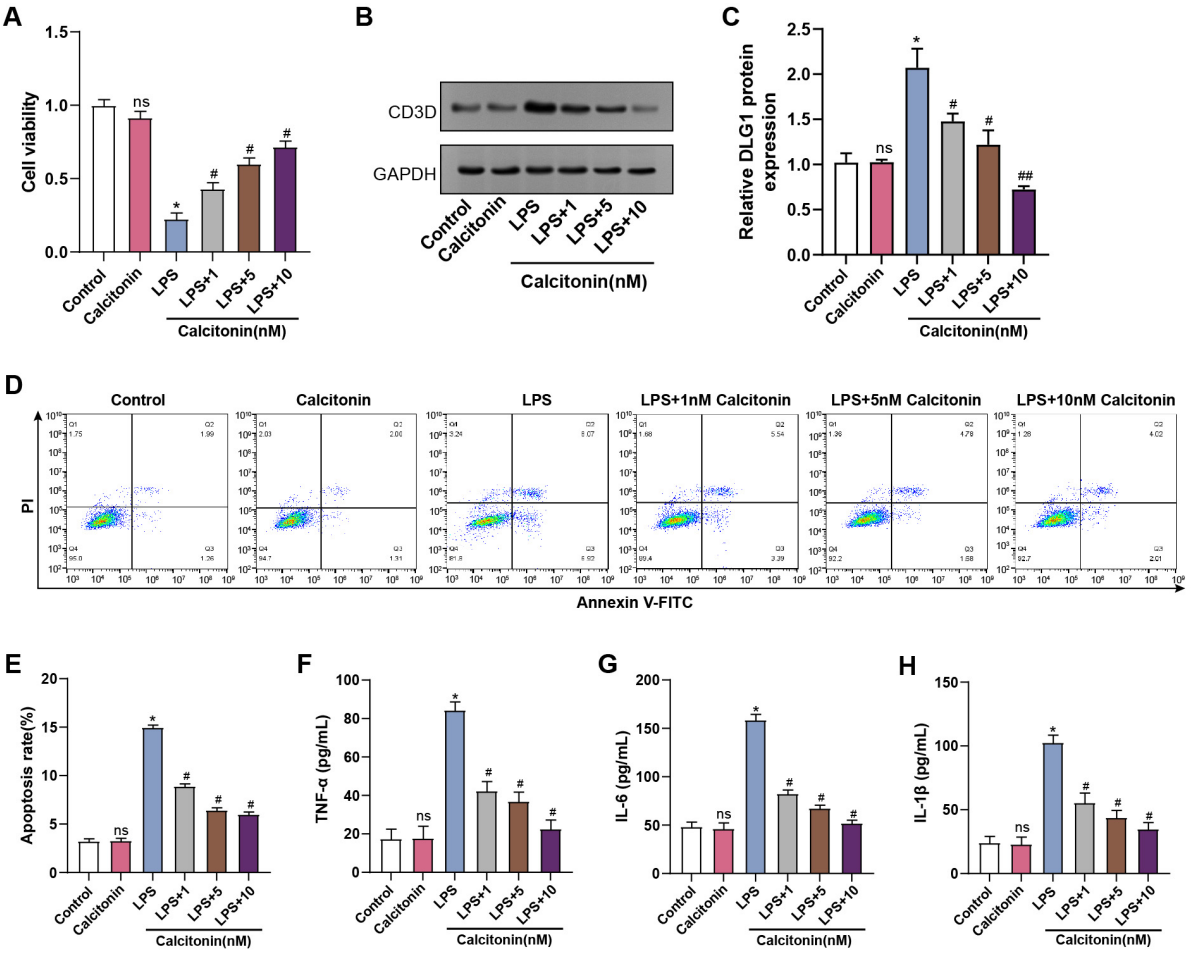

Fig. 7. Effect of calcitonin on cell viability, apoptosis, and inflammatory cytokine production in LPS-treated hPMECs. (A) Cell viability was assessed using CCK-8 assay after 24 hours of stimulation with LPS and treatment with different concentrations of calcitonin (1, 5, 10 nM). The y-axis represents the cell viability, and the x-axis represents different treatment conditions. (B) WB analysis of CD3D protein levels in hPMECs after 24 h of LPS stimulation and treatment with different concentrations of calcitonin (1, 5, 10 nM). (C) Quantification of CD3D protein expression levels from (B), normalized to GAPDH. (D) Flow cytometry plots showing apoptosis in hPMECs after 24 hours of stimulation with LPS and treatment with different concentrations of calcitonin (1, 5, 10 nM). (E) Quantification of the apoptosis rate in hPMECs under the indicated treatment conditions. (F) ELISA analysis of TNF-α expression levels in hPMECs following 24 hours of stimulation with LPS and treatment with different concentrations of calcitonin (1, 5, 10 nM). (G) ELISA analysis of IL-6 expression levels in hPMECs under the same treatment conditions. (H) ELISA analysis of IL-1β expression levels in hPMECs under the same treatment conditions. Each assay was performed in triplicate to ensure accuracy and reproducibility. Statistical significance was determined by comparing the mean values of each group. *$p < 0.05$ vs. Control group, $^{\#}p < 0.05$ vs. LPS group, $^{\#\#}p < 0.01$ vs. LPS group. ns vs. Control group.

3.9 Calcitonin Inhibits LPS-Induced Activation of the HMGB1/MyD88/NF-κB Pathway in hPMECs

To further explore the relationship between calcitonin and inflammatory signaling, the mRNA levels of key pathway components were assessed in hPMECs stimulated with LPS, with or without increasing concentrations of calcitonin. qRT-PCR analysis revealed that calcitonin alone did not alter *HMGB1*, *MyD88*, *NF-κB*, or *NLRP3* expression. LPS stimulation markedly increased *HMGB1*, *MyD88*, and *NLRP3*, whereas co-treatment with calcitonin suppressed this upregulation in a dose-dependent manner. *NF-κB* mRNA levels remained unchanged (Fig. 9A–D). WB analysis confirmed that calcitonin reduced LPS-induced expression of HMGB1, MyD88, NLRP3, and p-NF-κB (Fig. 9E,F).

3.10 Synergistic Effects of CD3D Knockdown and Calcitonin on Mitigating LPS-Induced Apoptosis and Enhancing Endothelial Viability in hPMECs

Among the investigated doses, 10 nM calcitonin had the most antioxidative impact and was thus chosen for further investigations. To determine the combined effect of *CD3D* knockdown and calcitonin, hPMECs were ex-

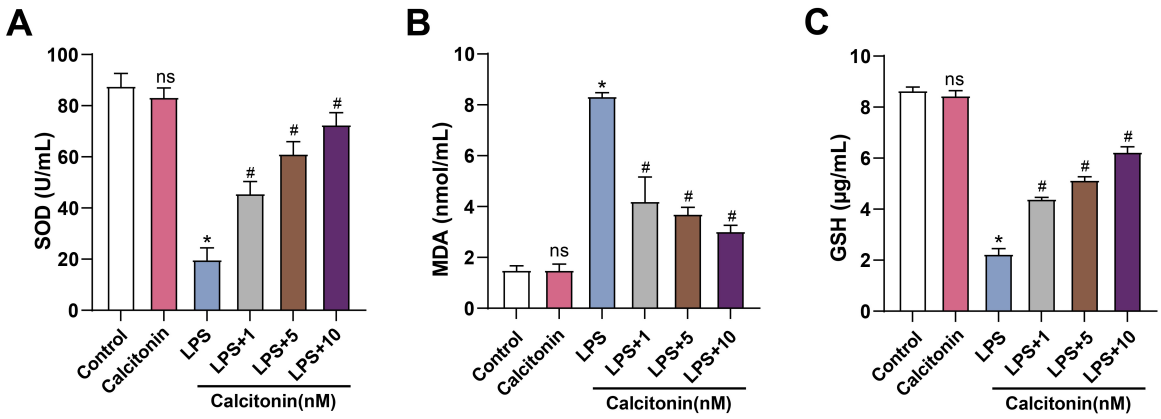

Fig. 8. Calcitonin modulates oxidative stress markers in LPS-stimulated hPMECs. (A) SOD activity in hPMECs was measured using a commercial SOD assay kit after 24 h of stimulation with 10 μg/mL LPS, with or without calcitonin treatment at concentrations of 1, 5, or 10 nM. The y-axis represents SOD activity (U/mL). (B) MDA levels in hPMECs were determined using a lipid peroxidation assay kit under the same treatment conditions. The y-axis represents MDA content (nmol/mL). (C) GSH levels in hPMECs were quantified using a GSH detection kit under the same treatment conditions. The y-axis represents GSH concentration (μg/mL). Each assay was performed in triplicate to ensure accuracy and reproducibility. Statistical significance was determined by comparing the mean values of each group. $^{*}p < 0.05$ vs. Control group, $^{\#}p < 0.05$ vs. LPS group. ns vs. Control group.

posed to LPS in the presence or absence of si-*CD3D*-2 and/or 10 nM calcitonin. CCK-8 assays showed that both *CD3D* knockdown and calcitonin treatment significantly restored LPS-impaired cell viability, while their combined application further enhanced viability, suggesting a synergistic effect (Fig. 10A). Flow cytometry confirmed that apoptosis was most effectively reduced in the co-treatment group (Fig. 10B). Both qRT-PCR and WB confirmed that combined therapy enhanced Bcl-2 levels while more effectively downregulating Bax and Caspase-3 compared to single-agent treatments (Fig. 10C–G). These data suggest that *CD3D* depletion and calcitonin act in concert to suppress LPS-triggered apoptosis and enhance endothelial resilience.

3.11 Combined CD3D Silencing and Calcitonin Treatment Synergistically Attenuates LPS-Induced Inflammation and Oxidative Stress in hPMECs

To further assess the regulatory effects of *CD3D* knockdown and calcitonin on inflammatory and oxidative responses in hPMECs under septic conditions, ELISA analysis was performed. *CD3D* knockdown substantially decreased LPS-induced TNF-α, IL-6, and IL-1β production, while co-treatment with calcitonin further enhanced this inhibitory effect (Fig. 11A–C). Similarly, oxidative stress analysis demonstrated that *CD3D* knockdown reduced MDA levels while restoring SOD and GSH, and co-treatment with calcitonin amplified these protective effects (Fig. 11D–F). Together, these results indicate that *CD3D* silencing, particularly in combination with calcitonin, effectively reduces LPS-induced inflammation and oxidative stress in hPMECs.

3.12 CD3D Knockdown Combined With Calcitonin Further Suppresses LPS-Induced HMGB1/MyD88/NF-κB Pathway Activation in hPMECs

To elucidate the underlying mechanisms, qRT-PCR analysis was performed. *CD3D* knockdown reduced LPS-induced expression of *HMGB1*, *MyD88*, and *NLRP3*, and co-treatment with calcitonin further enhanced this suppression, while *NF-κB* mRNA levels remained largely unaffected (Fig. 12A–D). WB analysis confirmed these results, showing that combined treatment with calcitonin and *CD3D* knockdown more effectively suppressed MyD88, HMGB1, NLRP3, and p-NF-κB compared with either therapy alone (Fig. 12E,F). These findings suggest that *CD3D* silencing and calcitonin synergistically protect against LPS-induced endothelial injury by inhibiting the HMGB1/MyD88/NF-κB pathway.

4. Discussion

Our research comprehensively explored the function of *CD3D* in sepsis and sepsis-induced ALI using bioinformatic analyses, clinical samples, and *in vitro* experiments. Analysis of sepsis-related transcriptomic datasets identified *CD3D* as a hub gene, characterized by elevated expression in sepsis and further upregulation in patients with ALI. Functional assays in hPMECs demonstrated that *CD3D* knockdown mitigated LPS-induced inflammatory responses, oxidative stress, cell cycle arrest, and apoptosis. Furthermore, calcitonin was shown to exert protective effects against LPS-induced endothelial injury in a dose-dependent manner. Importantly, combined treatment with *CD3D* knockdown and calcitonin produced synergistic effects in suppressing inflammation, oxidative stress, and HMGB1/MyD88/NF-κB pathway activation. Together,

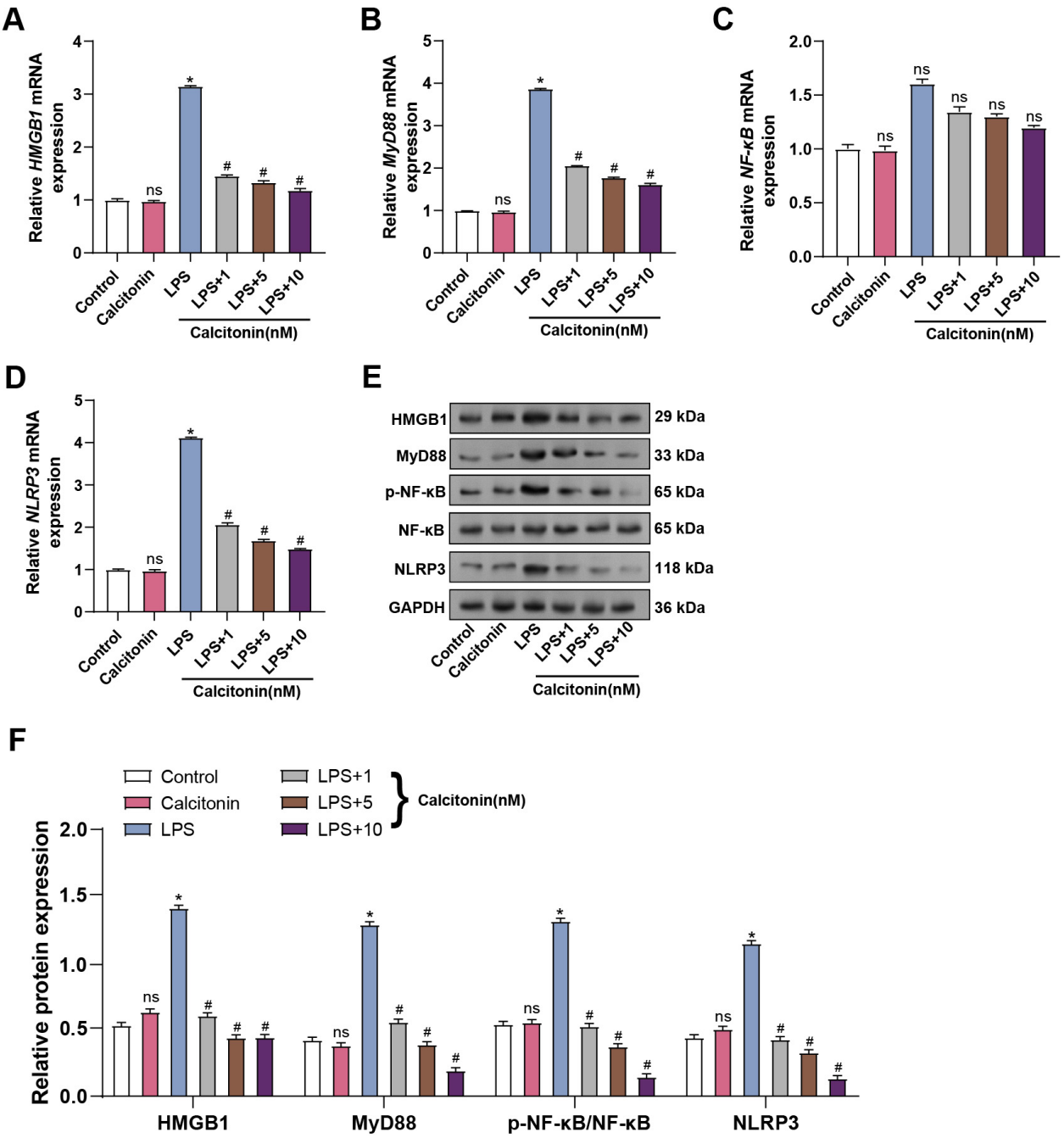

Fig. 9. Calcitonin attenuates LPS-induced inflammatory response via the NF-κB signaling pathway in hPMECs. (A) qRT-PCR analysis of *HMGB1* mRNA expression in hPMECs stimulated with 10 µg/mL LPS for 24 h, with or without calcitonin treatment (1, 5, 10 nM). (B) qRT-PCR analysis of *MyD88* mRNA expression under the same conditions. (C) qRT-PCR analysis of *NF-κB* mRNA expression under the same conditions. (D) qRT-PCR analysis of *NLRP3* mRNA expression under the same conditions. (E) Representative WB images showing protein levels of HMGB1, MyD88, p-NF-κB, NF-κB, and NLRP3 in hPMECs after LPS stimulation with or without calcitonin treatment. GAPDH served as the loading control. (F) Quantification of WB band intensities for HMGB1, MyD88, p-NF-κB/NF-κB, and NLRP3, normalized to GAPDH. *$p < 0.05$ vs. Control group, $^{\#}p < 0.05$ vs. LPS group. ns vs. Control group.

our findings demonstrate the pathogenic significance of *CD3D* in sepsis and suggest that *CD3D* targeting, either by itself or in conjunction with calcitonin, may be a viable therapeutic approach for ALI and endothelial dysfunction brought on by sepsis.

Sepsis can progress to severe infection and complications. Vigilant monitoring and management of organ dysfunction, circulatory failure, and metabolic disturbances are crucial therapeutic measures [23]. In this research, differential expression and functional enrichment analyses of

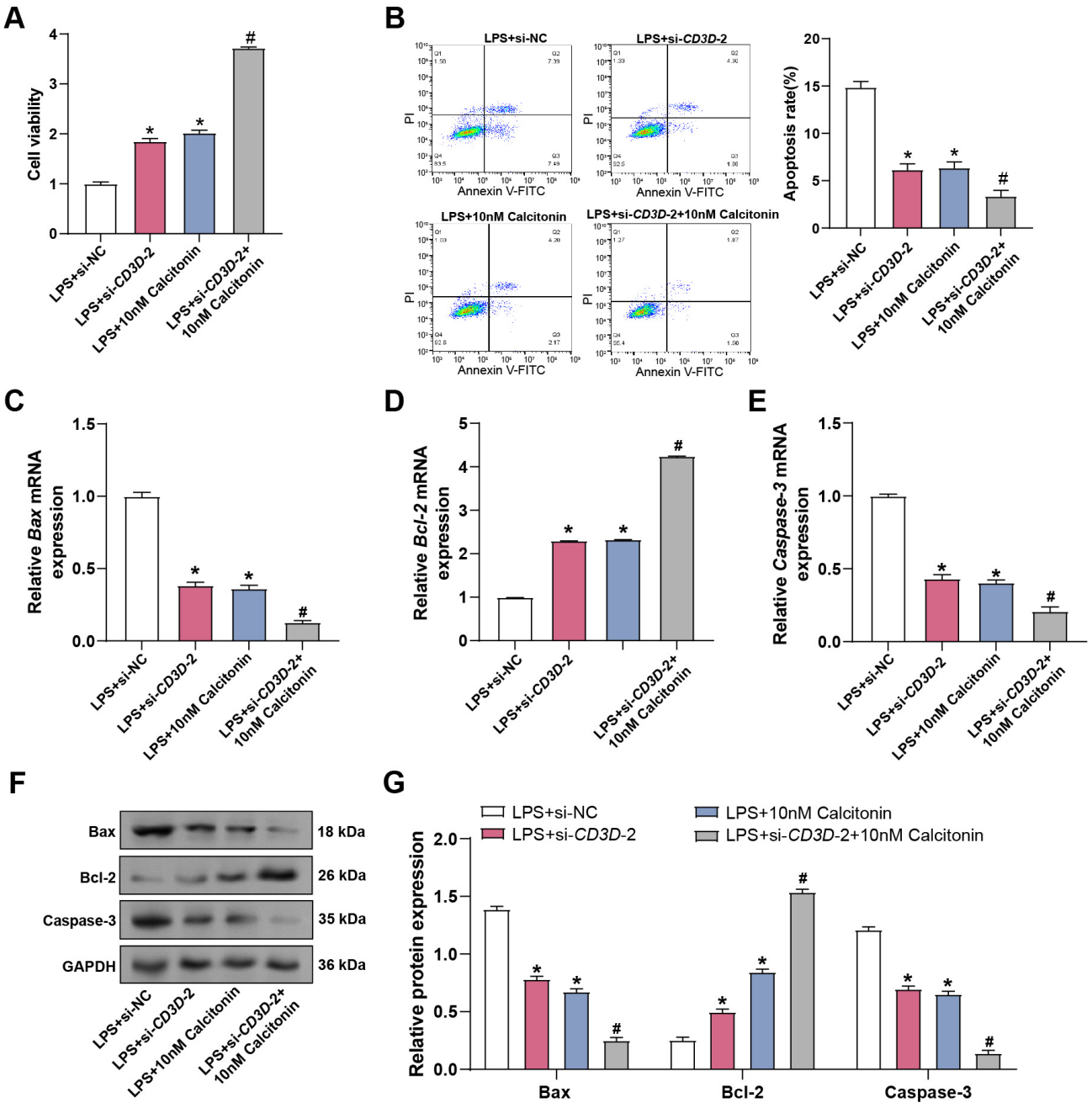

Fig. 10. Combined effect of calcitonin and *CD3D* silencing on LPS-induced viability and apoptosis in hPMECs. (A) Cell viability assessed by CCK-8 assay in hPMECs stimulated with LPS for 24 hours, co-treated with 10 nM calcitonin and subjected to *CD3D* knockdown. The x-axis represents different treatment conditions, and the y-axis represents cell viability. (B) Apoptosis was detected by flow cytometry in hPMECs stimulated with LPS for 24 hours, co-treated with 10 nM calcitonin, and subjected to *CD3D* knockdown. (C) qRT-PCR analysis of *Bax* mRNA levels in hPMECs stimulated with 10 µg/mL LPS for 24 hours, with or without *CD3D* knockdown and/or 10 nM calcitonin treatment. (D) qRT-PCR analysis of *Bcl-2* mRNA expression in hPMECs under the same conditions. (E) qRT-PCR analysis of *Caspase-3* mRNA expression in hPMECs under the same conditions. (F) Representative WB images showing protein expression levels of Bax, Bcl-2, and Caspase-3 in hPMECs under the same treatment conditions. GAPDH was used as an internal loading control. (G) Quantitative analysis of protein expression levels of Bax, Bcl-2, and Caspase-3 from WB results in (F), normalized to GAPDH. *$p < 0.05$ vs. LPS group, $^{\#}p < 0.05$ vs. LPS+10 nM Calcitonin group.

sepsis-related gene datasets were performed, identifying key pathways such as TCR Signaling Pathway, Calcium Channel Regulator Activity, and Endocytic Vesicle Membrane. Our study identified four significantly expressed

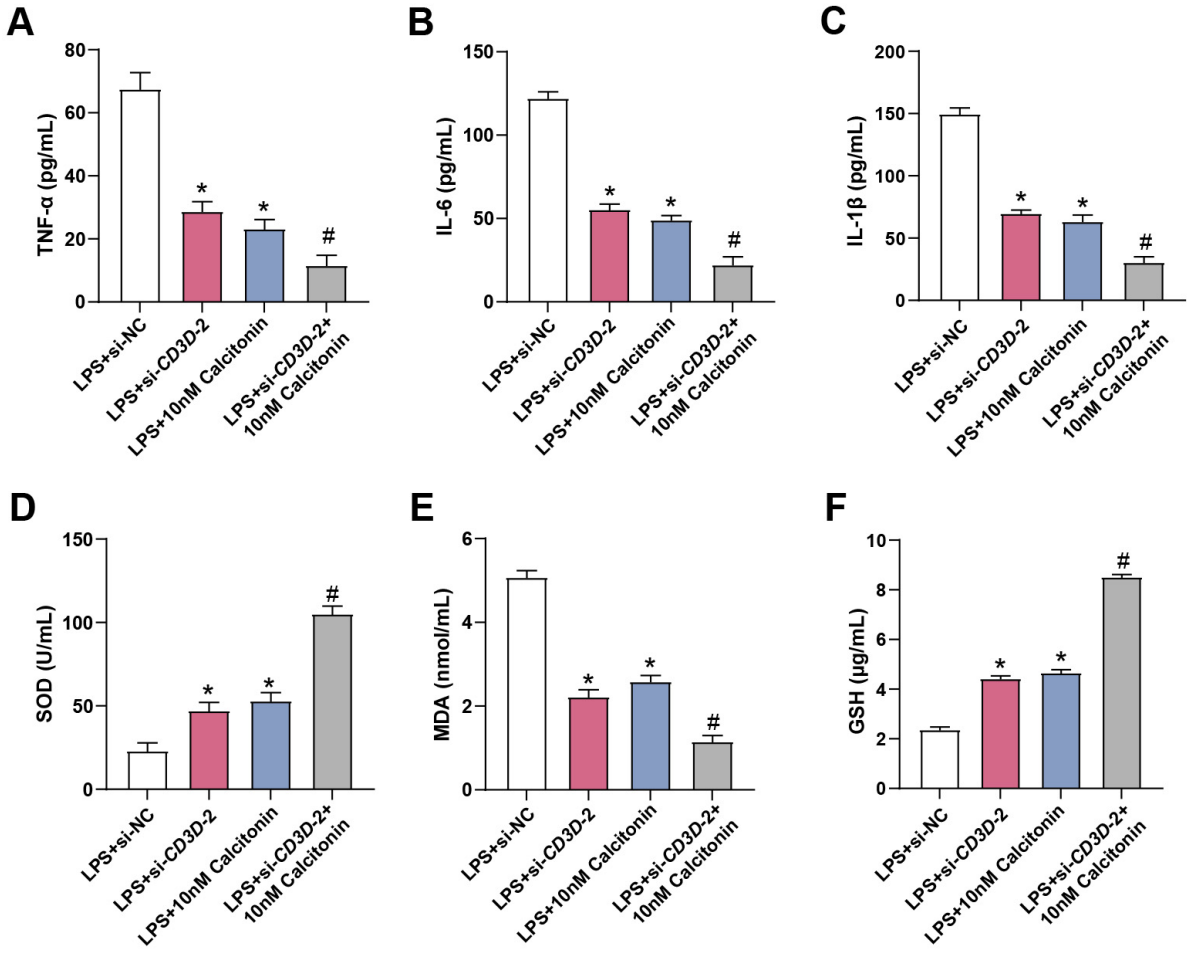

Fig. 11. Effects of calcitonin and *CD3D* knockdown on inflammatory cytokine production and oxidative stress in LPS-treated hPMECs. (A) ELISA analysis of TNF-α levels (pg/mL) in hPMECs exposed to 10 μg/mL LPS for 24 hours, with or without 10 nM calcitonin treatment and/or *CD3D* knockdown. (B) ELISA analysis of IL-6 levels (pg/mL) under the same treatment conditions. (C) ELISA analysis of IL-1β levels (pg/mL) under the same treatment conditions. (D) Measurement of SOD activity (U/mL) using a commercial detection kit in hPMECs exposed to LPS with or without calcitonin and/or *CD3D* knockdown. (E) Quantification of MDA content (nmol/mL) using a lipid peroxidation assay kit in the indicated groups. (F) Determination of GSH levels (μg/mL) in hPMECs treated with LPS, calcitonin, and/or *CD3D* knockdown. Experimental groups included LPS+si-NC, LPS+si-CD3D-2, LPS+10 nM calcitonin, and combined treatment with LPS+si-*CD3D*-2+10 Nm calcitonin. *$p < 0.05$ vs. LPS group, $^{\#}p < 0.05$ vs. LPS+10 nM Calcitonin group.

genes (*CCR7*, *CD247*, *CD3D*, and *CD69*) through PPI network analysis. Notably, Liang *et al.* [24] reported that *CCR7* and *CD3D* were closely linked to sepsis. Furthermore, Jiang *et al.* [25] found reduced expression of *FYN* and *CD247* in septic shock, connecting them to impaired immune responses and decreased T-cell activity. At the same time, Goswami *et al.* [26] identified *CD69* and *CD64* as upregulated markers for rapid sepsis detection. In this study, *CD3D* was identified as the most significantly differentially expressed gene across two independent sepsis-related datasets. *In vitro* experiments revealed that LPS stimulation markedly upregulated *CD3D* expression in hPMECs. LPS exposure induced G1 phase cell cycle arrest, whereas *CD3D* knockdown partially reversed this effect by downregulating *p21* and restoring the expression of *Cyclin D1* and *CDK2*, thereby facilitating cell cycle progression.

Immune cells emit important pro-inflammatory cytokines, such as TNF-α, IL-1β, and IL-6, in response to infection or tissue damage [27]. These mediators are crucial for controlling immune responses as well as coordinating the inflammatory cascade. Lee *et al.* [28] demonstrated a targeted delivery approach using the threonine–lysine–proline–arginine (TKPR)-nine arginine (9R) peptide to transport siRNA specifically into inflammation-associated macrophages. This strategy effectively silenced the TNF-α converting enzyme, thereby attenuating TNF-α activation and mitigating the downstream inflammatory response. In parallel, Liu and Chen [29] observed that higher

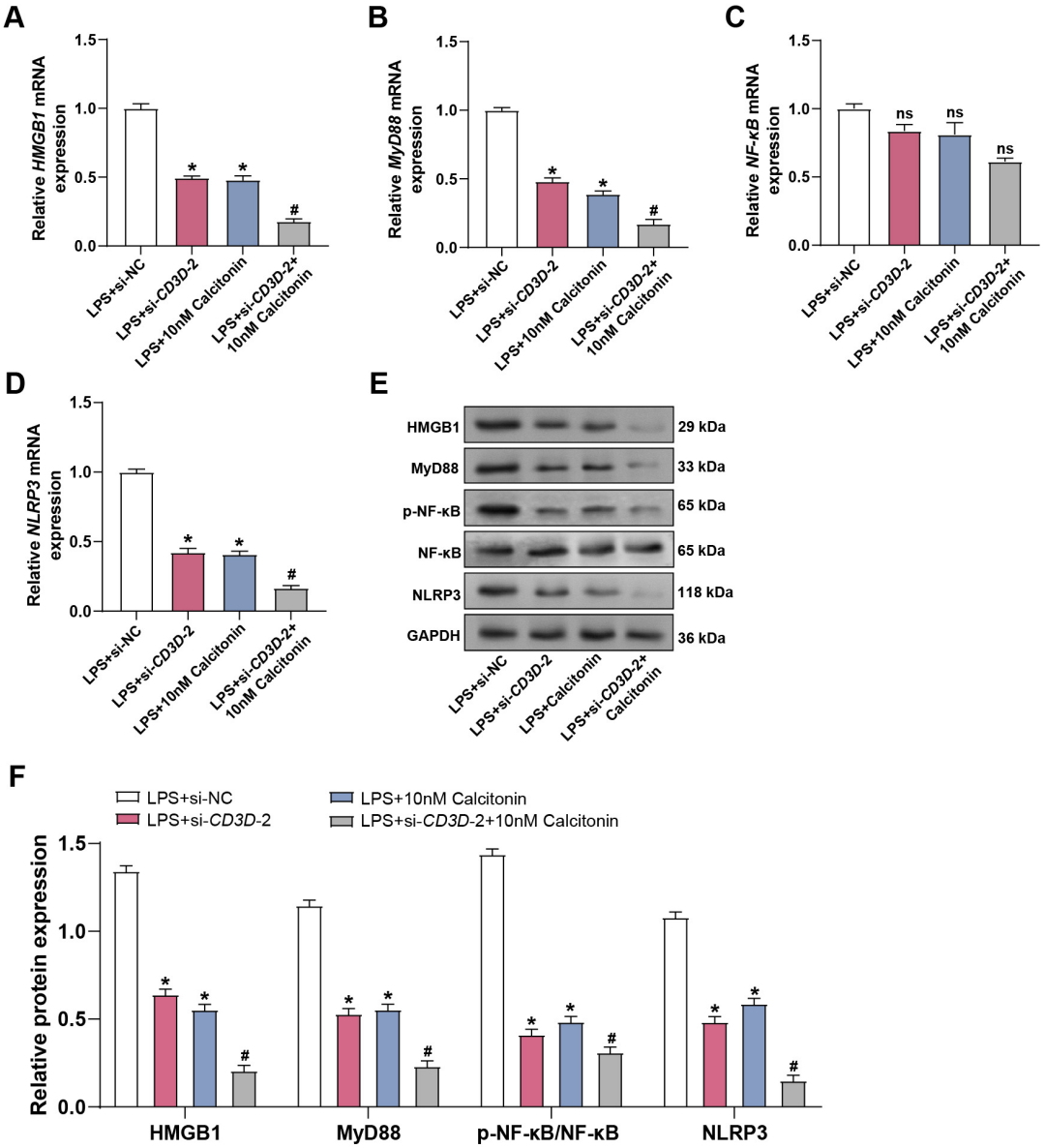

Fig. 12. *CD3D* knockdown combined with calcitonin suppresses LPS-induced activation of the HMGB1/MyD88/NF-κB/NLRP3 signaling pathway in hPMECs. (A) *HMGB1* mRNA expression in hPMECs measured by qRT-PCR after 24 h stimulation with 10 μg/mL LPS, with or without 10 nM calcitonin treatment and/or *CD3D* knockdown. (B) *MyD88* mRNA expression was detected under the same treatment conditions. (C) *NF-κB* mRNA expression was analyzed by qRT-PCR in the indicated groups. (D) *NLRP3* mRNA expression was measured under identical conditions. (E) Representative WB images of HMGB1, MyD88, NF-κB, p-NF-κB, and NLRP3 in hPMECs under the same treatments. GAPDH served as a loading control. (F) Quantification of WB results showing relative protein expression of HMGB1, MyD88, NF-κB/p-NF-κB, and NLRP3. *$p < 0.05$ vs. LPS group, $^{\#}p < 0.05$ vs. LPS+10 nM Calcitonin group. ns vs. LPS group or LPS+10 nM calcitonin group.

circulating IL-6 levels were significantly correlated with ALI and multiple organ dysfunction among septic patients. Furthermore, IL-6 concentrations have been shown to be positively correlated with illness severity, suggesting that it may be used as a biomarker for sepsis progression and the risk of complications. *COX-2* and *iNOS* are two enzymes commonly associated with inflammation, along with cellular stress. Zhang *et al.* [30] demonstrated that the specific inhibitor *PTUPB* inhibited *COX-2* and NLRP3 inflammasome activation in hepatic and pulmonary septic mice, thereby attenuating oxidative stress. Oliveira *et al.* [31] further emphasized that *iNOS* was markedly increased during sepsis, contributing to renal cortical shunting and medullary ischemia. Selective *iNOS* inhibition has thus been proposed as a potential strategy to mitigate sepsis-induced acute kidney injury. In line with these observations, our study re-

vealed that *CD3D* knockdown effectively reduced the secretion of TNF-α, IL-6, and IL-1β in LPS-stimulated hPMECs, thereby alleviating inflammation-induced growth inhibition. Additionally, *CD3D* knockdown reversed the LPS-induced activation of *COX-2* and *iNOS*. The data imply that *CD3D* contributes to controlling inflammation and oxidative stress during LPS-induced injury in hPMECs.

In sepsis, excessive release of bacterial endotoxins and cytokines leads to increased oxidative stress in the host organism. Oxidative stress plays a vital role in the development of sepsis, causing cellular damage and organ failure [32]. By preventing endoplasmic reticulum stress and enhancing mitochondrial activity, Sang *et al*. [33] showed that quercetin reduced oxidative stress damage and shielded mice against sepsis-induced ALI. Key indicators of cellular metabolism and oxidative stress, such as LDH, SOD, MDA, and GSH, are essential in disease research, providing insights into intracellular mechanisms. Liu *et al*. [34] further revealed that elevated LDH levels at admission were strongly related to increased 30-day mortality in septic patients. This finding underscores the potential of LDH as an important prognostic indicator for sepsis outcomes. Therapeutic strategies that focus on oxidative stress and inflammation have demonstrated promising effects in sepsis-induced ALI. Le *et al*. [35] demonstrated that N-acetylcysteine (NAC) mitigates ALI severity in septic rats by suppressing TNF-α and IL-1β, reducing oxidative stress markers such as MDA, and enhancing antioxidant enzyme activity, including SOD. Similarly, Xie *et al*. [36] revealed that pretreatment with lavender oil significantly attenuates ALI in septic models. These protective effects were characterized by reduced levels of inflammatory mediators and oxidative stress, decreased apoptosis, and enhanced antioxidant defenses.

Calcitonin has demonstrated strong anti-inflammatory properties in a range of inflammatory conditions, including sepsis [37]. Its ability to modulate the inflammatory response is critical for reducing tissue damage and improving survival rates in septic models. Baranowsky *et al*. [14] demonstrated that PCT exerts pro-inflammatory effects in sepsis-induced shock by acting through the CGPR receptor. This mechanism aggravates septic conditions by promoting immune cell production of the inflammatory cytokine IL-17A. In the present study, LPS stimulation of hPMECs exacerbated intracellular oxidative stress, as evidenced by increased MDA and LDH levels, along with reduced activities of the antioxidant enzymes SOD and GSH. Knockdown of the *CD3D* gene effectively reversed these alterations, thereby alleviating oxidative damage. Moreover, calcitonin exerted a dose-dependent protective effect against LPS-induced cellular injury, progressively restoring cell viability, reducing apoptosis, and significantly inhibiting the release of pro-inflammatory cytokines. Additionally, calcitonin reduced intracellular MDA levels while enhancing SOD and GSH content, collectively mitigating oxidative stress. Moreover, knockdown of *CD3D* also attenuated LPS-induced cytokine production and oxidative stress, and its combination with calcitonin further potentiated these protective effects, synergistically preserving pulmonary microvascular endothelial cells from injury.

In patients with sepsis and sepsis-induced ALI, serum analysis showed marked increases in CD3D, HMGB1, p-NF-κB, MyD88, as well as NLRP3, indicating that HMGB1/MyD88/NF-κB pathway activation may drive sepsis development and related lung inflammation. *HMGB1* and *MyD88* are crucial activators of the NF-κB pathway, which regulates inflammation and immune responses [38]. Dysregulated NF-κB activity has been linked to various inflammatory diseases and cancers, establishing it as a potential therapeutic target [39]. Evidence also indicates that calcitonin inhibits NF-κB signaling, thereby reducing inflammation and offering protective effects in sepsis [40]. Recent studies further demonstrated that calcitonin-related peptides alleviate sepsis-induced intestinal injury by suppressing NF-κB activation, reducing NLRP3 expression, and modulating cell adhesion proteins to limit inflammation. Moreover, NLRP3 is crucial in inflammasome formation and activation, as underscored by Danielski *et al*. [41], who demonstrated its role in promoting caspase-1 activation, leading to the maturation and release of IL-1β and IL-18, thereby exacerbating inflammatory responses. LPS stimulation significantly upregulated levels of *HMGB1*, *MyD88*, *NF-κB*, and *NLRP3* in hPMECs. Calcitonin inhibited this upregulation in a concentration-dependent manner, thereby attenuating the inflammatory response. Similarly, *CD3D* knockdown suppressed these inflammatory mediators, while combined treatment with calcitonin produced a more pronounced inhibitory effect. These findings suggest that calcitonin and *CD3D* knockdown synergistically mitigate LPS-induced inflammation in pulmonary microvascular endothelial cells through modulation of the HMGB1/MyD88/NF-κB pathway.

Our study demonstrates that both calcitonin treatment and *CD3D* knockdown reduce inflammatory and oxidative stress responses *in vitro*. However, the precise mechanistic relationship between calcitonin and *CD3D* remains unclear. It is not yet determined whether calcitonin directly modulates *CD3D* expression or whether these interventions act through distinct, convergent pathways to achieve similar protective effects. Further molecular investigations are warranted to clarify this relationship and to elucidate the signaling cascades involved. From a clinical perspective, the *in vitro* concentrations of calcitonin used in this study (1–10 nM) exhibited pronounced protective effects. Nevertheless, it remains uncertain whether such concentrations can be safely achieved in patients. Careful evaluation of dosing strategies, pharmacokinetics, and potential side effects is therefore essential before clinical translation. Moreover, the present study was primarily conducted *in vitro*, which may not fully recapitulate the complex immune and

metabolic environment of sepsis *in vivo*. Additionally, the patient serum analysis included an extremely small sample size (n = 3 per group), which is insufficient for drawing robust statistical conclusions and substantially limits the generalizability of our findings. Although Cohen's d effect sizes were reported to better illustrate the magnitude of group differences, the confidence intervals for several comparisons were wide, reflecting the limited precision caused by the small sample size. This further underscores the need for cautious interpretation and highlights that these preliminary findings should be validated in larger and independent patient cohorts to yield more stable effect size estimates and narrower confidence intervals. The reported dual role of calcitonin in other contexts, including potential pro-inflammatory effects, further underscores the need for cautious interpretation. Future studies with larger patient cohorts and *in vivo* models are necessary to validate our findings and to optimize therapeutic strategies for targeting inflammation and oxidative stress in sepsis.

5. Conclusion

In conclusion, this study identifies *CD3D* as a key pro-inflammatory mediator contributing to endothelial dysfunction in sepsis and sepsis-induced ALI. Functional experiments demonstrated that *CD3D* knockdown alleviated LPS-induced inflammation, cell cycle arrest, and oxidative stress in hPMECs. Concurrently, calcitonin exhibited dose-dependent protective effects against LPS-induced injury, including the suppression of inflammatory cytokine production, oxidative damage, and apoptosis. Notably, combined *CD3D* silencing and calcitonin treatment exerted synergistic benefits by further restoring endothelial viability and suppressing activation of the HMGB1/MyD88/NF-κB pathway and NLRP3 inflammasome. Collectively, the data highlight *CD3D* as a key regulator of endothelial injury in sepsis, pointing to calcitonin as a potential adjunct therapy.

Availability of Data and Materials

The datasets used and analyzed in this article are accessible from the corresponding author upon reasonable request.

Author Contributions

Conception and design: HZ, RZ, JH; Data acquisition: RZ, HW; Data analysis: HZ, RZ, JJ, HW; Manuscript drafting: HZ, RZ; Critical revision: All authors contributed to editorial changes in the manuscript. All authors read and approved the final manuscript. All authors have participated sufficiently in the work and agreed to be accountable for all aspects of the work.

Ethics Approval and Consent to Participate

Our study is approved by Academic Committee of the Third Affiliated Hospital of Naval Medical University (approval number: KY2024081). All participants and their legal guardians provided written informed consent. The study was carried out in accordance with the guidelines of the Declaration of Helsinki.

Acknowledgment

Not applicable.

Funding

This research was supported by the research on the mechanism of alveolar epithelial cell-derived exosomes loaded with Isthmin-1 in regulating pulmonary capillary leakage in sepsis (2023 QN098) and the research on the mechanism of alveolar epithelial cell-derived exosomes loaded with Isthmin-1 in regulating pulmonary capillary leakage in sepsis (2023 QN008).

Conflict of Interest

The authors declare no conflict of interest.

Declaration of AI and AI-Assisted Technologies in the Writing Process

In this dissertation, the authors used AI tools to assist in literature retrieval and organization/diagram and audio/video production/code debugging and analysis/grammar proofreading and format checking, etc. The core ideas, research design, conclusions and innovations of the dissertation were all completed independently by us. We conducted a legal review and reasonable editing of the content completed with the assistance of this tool, and I assume all legal and academic ethical responsibilities for the content of this dissertation.

References

[1] Ibarz M, Haas LEM, Ceccato A, Artigas A. The critically ill older patient with sepsis: a narrative review. Annals of Intensive Care. 2024; 14: 6. https://doi.org/10.1186/s13613-023-01233-7.

[2] Sun B, Lei M, Zhang J, Kang H, Liu H, Zhou F. Acute lung injury caused by sepsis: how does it happen? Frontiers in Medicine. 2023; 10: 1289194. https://doi.org/10.3389/fmed.2023.1289194.

[3] Qiao X, Yin J, Zheng Z, Li L, Feng X. Endothelial cell dynamics in sepsis-induced acute lung injury and acute respiratory distress syndrome: pathogenesis and therapeutic implications. Cell Communication and Signaling. 2024; 22: 241. https://doi.org/10.1186/s12964-024-01620-y.

[4] Joffre J, Hellman J. Oxidative Stress and Endothelial Dysfunction in Sepsis and Acute Inflammation. Antioxidants & Redox Signaling. 2021; 35: 1291–1307. https://doi.org/10.1089/ars.2021.0027.

[5] Tang F, Zhao XL, Xu LY, Zhang JN, Ao H, Peng C. Endothelial dysfunction: Pathophysiology and therapeutic targets for sepsis-induced multiple organ dysfunction syndrome. Biomedicine & Pharmacotherapy. 2024; 178: 117180. https://doi.org/10.1016/j.biopha.2024.117180.

[6] Dikmen N, Cellat M, Etyemez M, İşler CT, Uyar A, Aydın T, *et al*. Ameliorative Effects of Oleuropein on Lipopolysaccharide-

Induced Acute Lung Injury Model in Rats. Inflammation. 2021; 44: 2246–2259. https://doi.org/10.1007/s10753-021-01496-x.

[7] Wang S, Luo SX, Jie J, Li D, Liu H, Song L. Efficacy of terpenoids in attenuating pulmonary edema in acute lung injury: A meta-analysis of animal studies. Frontiers in Pharmacology. 2022; 13: 946554. https://doi.org/10.3389/fphar.2022.946554.

[8] Kumar S, Saxena J, Srivastava VK, Kaushik S, Singh H, Abo-El-Sooud K, *et al*. The Interplay of Oxidative Stress and ROS Scavenging: Antioxidants as a Therapeutic Potential in Sepsis. Vaccines. 2022; 10: 1575. https://doi.org/10.3390/vaccines10101575.

[9] Üstündağ H. The role of antioxidants in sepsis management: a review of therapeutic applications. Eurasian Journal of Molecular and Biochemical Sciences. 2023; 2: 38–48.

[10] Zaki HA, Bensliman S, Bashir K, Iftikhar H, Fayed MH, Salem W, *et al*. Accuracy of procalcitonin for diagnosing sepsis in adult patients admitted to the emergency department: a systematic review and meta-analysis. Systematic Reviews. 2024; 13: 37. https://doi.org/10.1186/s13643-023-02432-w.

[11] Xu HG, Tian M, Pan SY. Clinical utility of procalcitonin and its association with pathogenic microorganisms. Critical Reviews in Clinical Laboratory Sciences. 2022; 59: 93–111. https://doi.org/10.1080/10408363.2021.1988047.

[12] Singh S, Kabra A, Goyal P. Physiological and therapeutic role of calcitonin. Research Journal of Pharmacy and Technology. 2024; 17: 1881–1884. https://doi.org/10.52711/0974-360X.2024.00298.

[13] Liu Y, Zheng Y, Ding S. The correlation between serum calcium levels and prognosis in patients with severe acute osteomyelitis. Frontiers in Immunology. 2024; 15: 1378730. https://doi.org/10.3389/fimmu.2024.1378730.

[14] Baranowsky A, Appelt J, Kleber C, Lange T, Ludewig P, Jahn D, *et al*. Procalcitonin Exerts a Mediator Role in Septic Shock Through the Calcitonin Gene-Related Peptide Receptor. Critical Care Medicine. 2021; 49: e41–e52. https://doi.org/10.1097/CCM.0000000000004731.

[15] Liu D, Hu X, Chen Z, Wei W, Wu Y. Key links in the physiological regulation of the immune system and disease induction: T cell receptor -CD3 complex. Biochemical Pharmacology. 2024; 227: 116441. https://doi.org/10.1016/j.bcp.2024.116441.

[16] Garcillán B, Fuentes P, Marin AV, Megino RF, Chacon-Arguedas D, Mazariegos MS, *et al*. *CD3G* or *CD3D* Knockdown in Mature, but Not Immature, T Lymphocytes Similarly Cripples the Human TCR$\alpha\beta$ Complex. Frontiers in Cell and Developmental Biology. 2021; 9: 608490. https://doi.org/10.3389/fcell.2021.608490.

[17] Li X, Chen Z, Yao Y, Chen M, Hu Y. Single-Cell Multi-Omics Deciphers Core Gene Networks and Immune Interaction Collapse in Sepsis-Associated T Cell Dysfunction. Infection and Drug Resistance. 2025; 18: 4863-4885. https://doi.org/10.2147/IDR.S538883.

[18] Yang Q, Feng Z, Ding D, Kang C. CD3D and CD247 are the molecular targets of septic shock. Medicine. 2023; 102: e34295. https://doi.org/10.1097/MD.0000000000034295.

[19] Moskot M, Jakóbkiewicz-Banecka J, Kloska A, Piotrowska E, Narajczyk M, Gabig-Cimińska M. The Role of Dimethyl Sulfoxide (DMSO) in Gene Expression Modulation and Glycosaminoglycan Metabolism in Lysosomal Storage Disorders on an Example of Mucopolysaccharidosis. International Journal of Molecular Sciences. 2019; 20: 304. https://doi.org/10.3390/ijms20020304.

[20] Zhang C, Wang H, Wang H, Shi S, Zhao P, Su Y, *et al*. A microsatellite DNA-derived oligodeoxynucleotide attenuates lipopolysaccharide-induced acute lung injury in mice by inhibiting the HMGB1-TLR4-NF-κB signaling pathway. Frontiers in Microbiology. 2022; 13: 964112. https://doi.org/10.3389/fmicb.2022.964112.

[21] Xiao Y, Zhang B, Hou S, Shen X, Wu X, Liu R, *et al*. Acacetin Attenuates Sepsis-induced Acute Lung Injury via NLRC3-NF-κB Pathway. Inflammation. 2025; 48: 75–88. https://doi.org/10.1007/s10753-024-02040-3.

[22] Kiriakopoulos A, Giannakis P, Menenakos E. Calcitonin: current concepts and differential diagnosis. Therapeutic Advances in Endocrinology and Metabolism. 2022; 13: 20420188221099344. https://doi.org/10.1177/20420188221099344.

[23] Kumbhar SM, Patil Y. Sepsis and septic shock: an update on clinical management and outcomes. In Obstetrics & Gynaecology Forum. 2024.

[24] Liang G, Li J, Pu S, He Z. Screening of Sepsis Biomarkers Based on Bioinformatics Data Analysis. Journal of Healthcare Engineering. 2022; 2022: 6788569. https://doi.org/10.1155/2022/6788569.

[25] Jiang Y, Miao Q, Hu L, Zhou T, Hu Y, Tian Y. *FYN* and *CD247*: Key Genes for Septic Shock Based on Bioinformatics and Meta-Analysis. Combinatorial Chemistry & High Throughput Screening. 2022; 25: 1722–1730. https://doi.org/10.2174/1386207324666210816123508.

[26] Goswami DG, Garcia LF, Dodoo C, Dwivedi AK, Zhou Y, Pappas D, *et al*. Evaluating the Timeliness and Specificity of CD69, CD64, and CD25 as Biomarkers of Sepsis in Mice. Shock. 2021; 55: 507–518. https://doi.org/10.1097/SHK.0000000000001650.

[27] Tylutka A, Walas Ł, Zembron-Lacny A. Level of IL-6, TNF, and IL-1β and age-related diseases: a systematic review and meta-analysis. Frontiers in Immunology. 2024; 15: 1330386. https://doi.org/10.3389/fimmu.2024.1330386.

[28] Lee J, Son W, Hong J, Song Y, Yang CS, Kim YH. Down-regulation of TNF-α via macrophage-targeted RNAi system for the treatment of acute inflammatory sepsis. Journal of Controlled Release. 2021; 336: 344–353. https://doi.org/10.1016/j.jconrel.2021.06.022.

[29] Liu Y, Chen L. Impact of interleukin 6 levels on acute lung injury risk and disease severity in critically ill sepsis patients. World Journal of Clinical Cases. 2024; 12: 5374–5381. https://doi.org/10.12998/wjcc.v12.i23.5374.

[30] Zhang YF, Sun CC, Duan JX, Yang HH, Zhang CY, Xiong JB, *et al*. A COX-2/sEH dual inhibitor PTUPB ameliorates cecal ligation and puncture-induced sepsis in mice via anti-inflammation and anti-oxidative stress. Biomedicine & Pharmacotherapy. 2020; 126: 109907. https://doi.org/10.1016/j.biopha.2020.109907.

[31] Oliveira FRMB, Assreuy J, Sordi R. The role of nitric oxide in sepsis-associated kidney injury. Bioscience Reports. 2022; 42: BSR20220093. https://doi.org/10.1042/BSR20220093.

[32] Karimi A, Naeini F, Niazkar HR, Tutunchi H, Musazadeh V, Mahmoodpoor A, *et al*. Nano-curcumin supplementation in critically ill patients with sepsis: a randomized clinical trial investigating the inflammatory biomarkers, oxidative stress indices, endothelial function, clinical outcomes and nutritional status. Food & Function. 2022; 13: 6596–6612. https://doi.org/10.1039/d1fo03746c.

[33] Sang A, Wang Y, Wang S, Wang Q, Wang X, Li X, *et al*. Quercetin attenuates sepsis-induced acute lung injury via suppressing oxidative stress-mediated ER stress through activation of SIRT1/AMPK pathways. Cellular Signalling. 2022; 96: 110363. https://doi.org/10.1016/j.cellsig.2022.110363.

[34] Liu Z, Liu F, Liu C, Chen X. Association between Lactate Dehydrogenase and 30-Day Mortality in Patients with Sepsis: a Retrospective Cohort Study. Clinical Laboratory. 2023; 69: 10.7754/Clin.Lab.2022.220915. https://doi.org/10.7754/Clin.Lab.2022.220915.

[35] Le JW, Sun M, Zhu JH, Fan H. Protective effect of N-acetylcysteine on acute lung injury in septic rats by inhibiting inflammation, oxidation, and apoptosis. Iranian Journal of Basic Medical Sciences. 2022; 25: 859–864. https://doi.org/10.22038/IJBMS.2022.65350.14384.

[36] Xie Q, Wang Y, Zou GL. Protective effects of lavender oil on sepsis-induced acute lung injury via regulation of the NF-κB pathway. Pharmaceutical Biology. 2022; 60: 968–978. https://doi.org/10.1080/13880209.2022.2067570.

[37] Bonura A, Brunelli N, Marcosano M, Iaccarino G, Fofi L, Vernieri F, *et al*. Calcitonin Gene-Related Peptide Systemic Effects: Embracing the Complexity of Its Biological Roles-A Narrative Review. International Journal of Molecular Sciences. 2023; 24: 13979. https://doi.org/10.3390/ijms241813979.

[38] Liu X, Lu B, Fu J, Zhu X, Song E, Song Y. Amorphous silica nanoparticles induce inflammation via activation of NLRP3 inflammasome and HMGB1/TLR4/MYD88/NF-kb signaling pathway in HUVEC cells. Journal of Hazardous Materials. 2021; 404: 124050. https://doi.org/10.1016/j.jhazmat.2020.124050.

[39] Zhang T, Ma C, Zhang Z, Zhang H, Hu H. NF-κB signaling in inflammation and cancer. MedComm. 2021; 2: 618–653. https://doi.org/10.1002/mco2.104.

[40] Becker KL, Nylén ES, White JC, Müller B, Snider RH, Jr. Clinical review 167: Procalcitonin and the calcitonin gene family of peptides in inflammation, infection, and sepsis: a journey from calcitonin back to its precursors. The Journal of Clinical Endocrinology and Metabolism. 2004; 89: 1512–1525. https://doi.org/10.1210/jc.2002-021444.

[41] Danielski LG, Giustina AD, Bonfante S, Barichello T, Petronilho F. The NLRP3 Inflammasome and Its Role in Sepsis Development. Inflammation. 2020; 43: 24–31. https://doi.org/10.1007/s10753-019-01124-9.